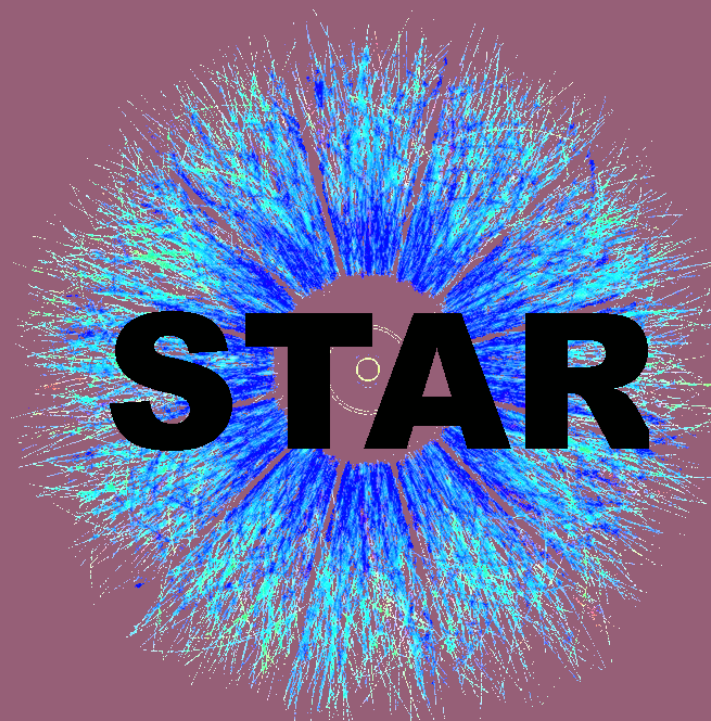




**Faculty
of Physics**

WARSAW UNIVERSITY OF TECHNOLOGY



Femtoscopic measurements of two-kaon combinations in Au+Au collisions at the STAR experiment

Diana Pawłowska (for the STAR Collaboration)

diana.pawlowska.dokt@pw.edu.pl

**Strangeness in Quark Matter 2022,
Busan, Republic of Korea,**

13-19 June 2022



Partially funded by:

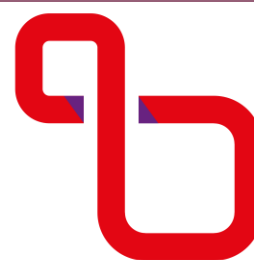


U.S. DEPARTMENT OF
ENERGY

Office of
Science



NATIONAL SCIENCE CENTRE
POLAND



RESEARCH
UNIVERSITY
EXCELLENCE INITIATIVE



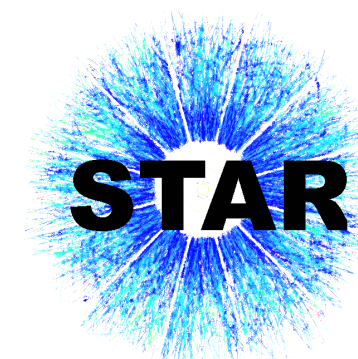
Femtoscscopy - introduction

$$CF(\vec{q}) = \frac{P_{12}(\vec{p}_1, \vec{p}_2)}{P_1(\vec{p}_1)P_2(\vec{p}_2)} = \int d^3r S(\vec{q}, \vec{r}) |\Psi(\vec{q}, \vec{r})|^2 = \frac{A(\vec{q})}{B(\vec{q})}$$

\vec{p}_1, \vec{p}_2 - single particle momentum

$S(\vec{q}, \vec{r})$ - emission function
 $\Psi(\vec{q}, \vec{r})$ - pair wave function
 $\vec{q} = |\vec{p}_1 - \vec{p}_2|$ - relative momentum
 \vec{r} - relative distance between two particles

$A(\vec{q})$ - correlated
 $B(\vec{q})$ - uncorrelated



Femtoscscopy - introduction

$$CF(\vec{q}) = \frac{P_{12}(\vec{p}_1, \vec{p}_2)}{P_1(\vec{p}_1)P_2(\vec{p}_2)} = \int d^3r S(\vec{q}, \vec{r}) |\Psi(\vec{q}, \vec{r})|^2 = \frac{A(\vec{q})}{B(\vec{q})}$$

\vec{p}_1, \vec{p}_2 - single particle momentum

$S(\vec{q}, \vec{r})$ - emission function

$A(\vec{q})$ - correlated

$\Psi(\vec{q}, \vec{r})$ - pair wave function

$B(\vec{q})$ - uncorrelated

$\vec{q} = |\vec{p}_1 - \vec{p}_2|$ - relative momentum

\vec{r} - relative distance between two particles

Kaon correlation functions are sensitive to:

$K^\pm K^\pm$

$K_s^0 K_s^0$

$K_s^0 K^\pm$

Quantum Statistical effects
(QS)

Quantum Statistical effects
(QS)

Final State Interaction
(FSI)

Final State Interaction (FSI)
- Coulomb interaction
(COUL)

Final State Interaction (FSI)
- strong interaction (SI)

- strong interaction (SI)



Femtoscscopy - introduction

$$CF(\vec{q}) = \frac{P_{12}(\vec{p}_1, \vec{p}_2)}{P_1(\vec{p}_1)P_2(\vec{p}_2)} = \int d^3r S(\vec{q}, \vec{r}) |\Psi(\vec{q}, \vec{r})|^2 = \frac{A(\vec{q})}{B(\vec{q})}$$

\vec{p}_1, \vec{p}_2 - single particle momentum

$S(\vec{q}, \vec{r})$ - emission function

$A(\vec{q})$ - correlated

$\Psi(\vec{q}, \vec{r})$ - pair wave function

$B(\vec{q})$ - uncorrelated

$\vec{q} = |\vec{p}_1 - \vec{p}_2|$ - relative momentum

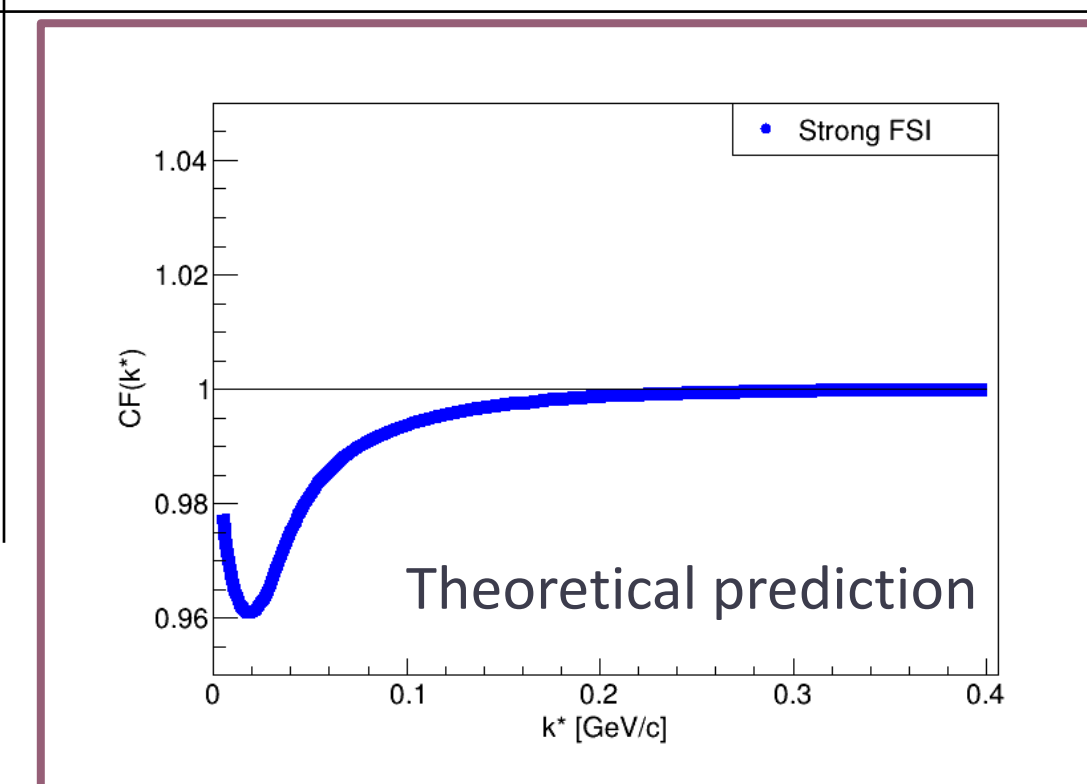
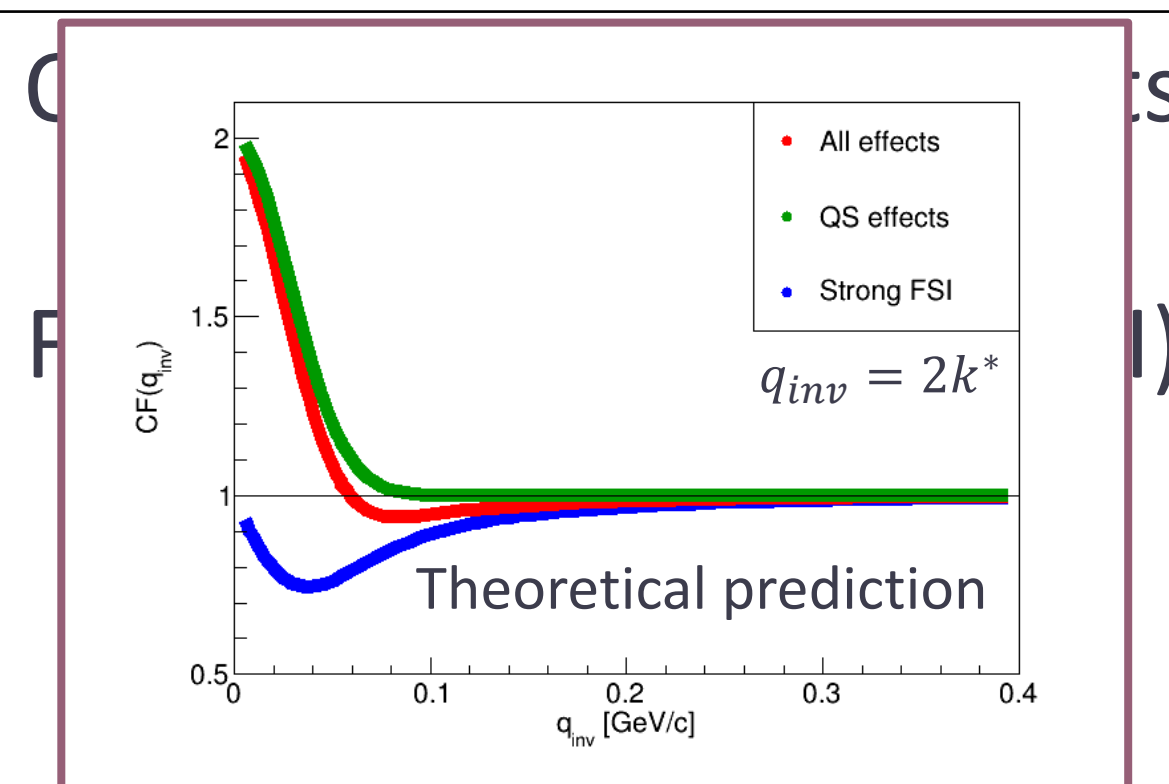
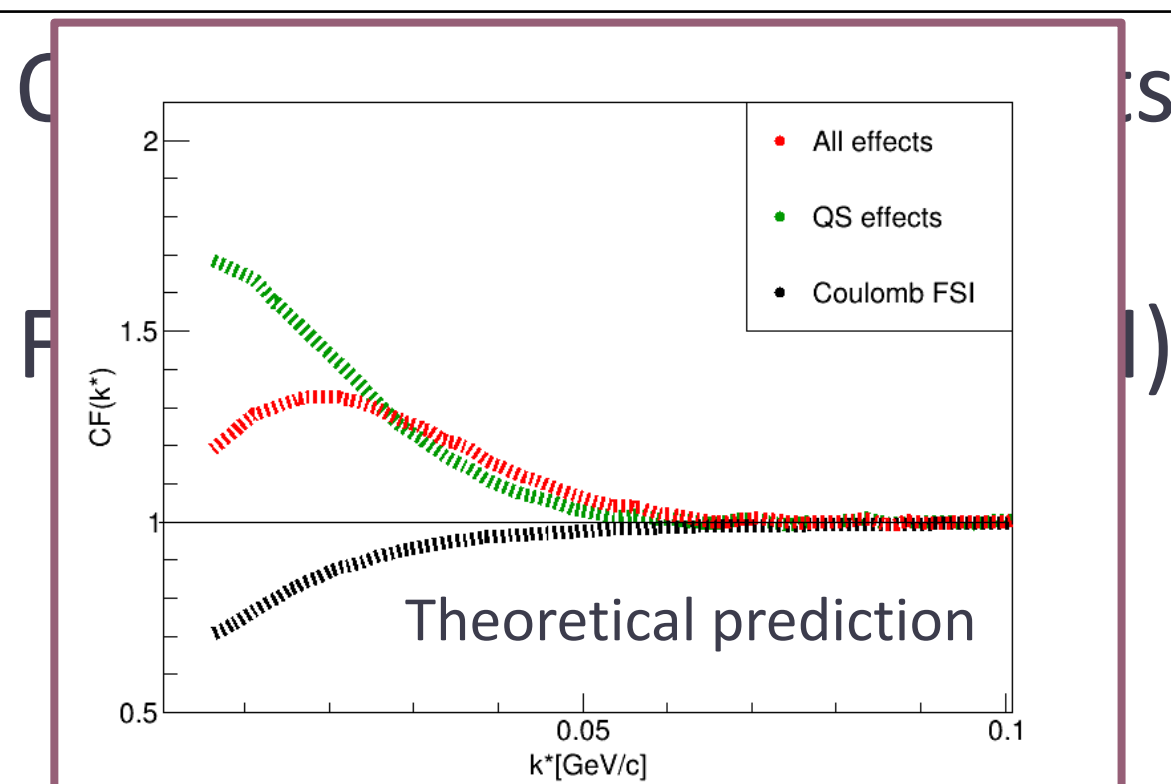
\vec{r} - relative distance between two particles

Kaon correlation functions are sensitive to:

$K^\pm K^\pm$

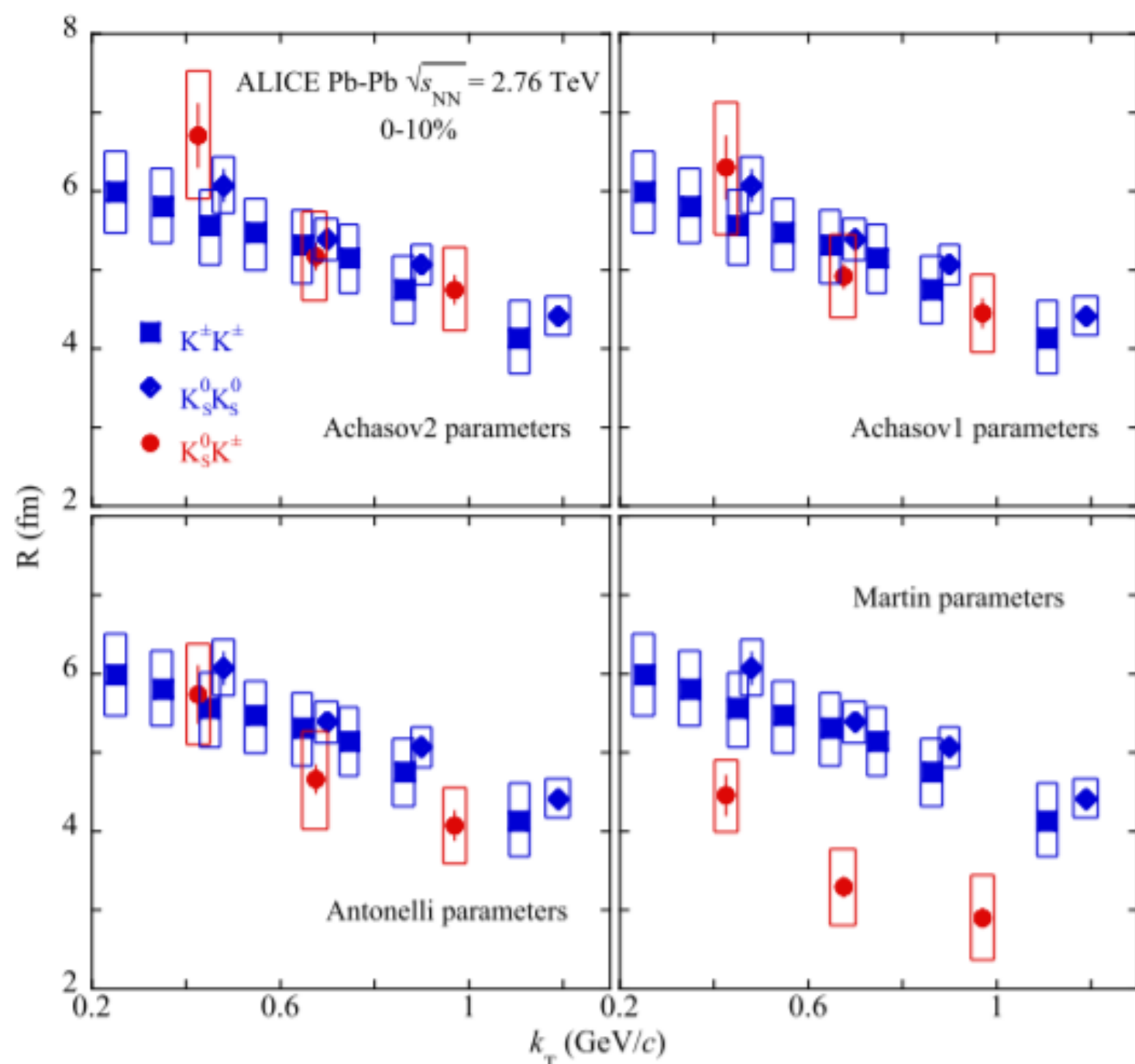
$K_S^0 K_S^0$

$K_S^0 K^\pm$



Motivation

ALICE, Physics Letters B **774**(2017) 64



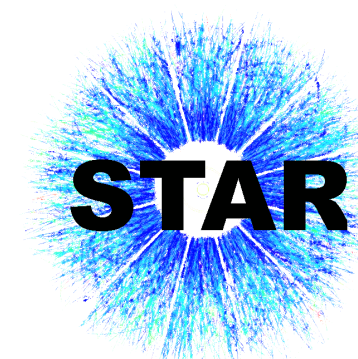
$$k_T = \frac{p_{T1} + p_{T2}}{2}$$

Kaons provide complementary information to pions:

- contain strange quarks (larger production of strange particles is one of the signatures of QGP)
- less affected by the feed-down from resonance decays
- smaller cross section on reaction with the hadronic matter

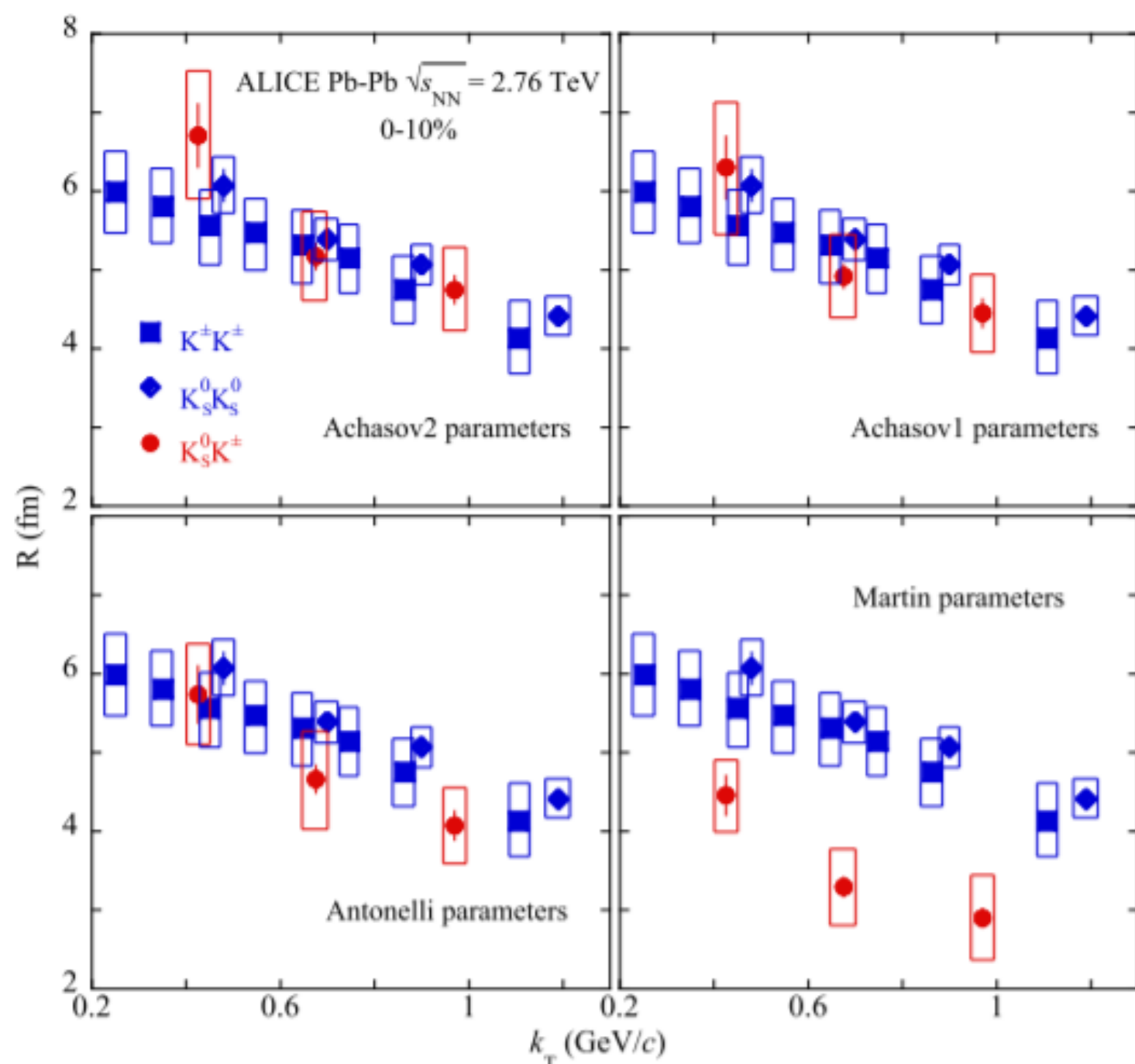
Very interesting:

- compare femtoscopic results for all possible kaon combination ($K^\pm K^\pm$, $K_S^0K_S^0$, $K_S^0K^\pm$)
- $K_S^0K^\pm$ - a_0 could be a 4-quark state (a tetraquark)



Motivation

ALICE, Physics Letters B **774**(2017) 64



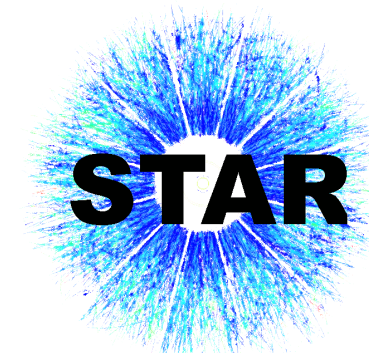
$$k_T = \frac{p_{T1} + p_{T2}}{2}$$

Kaons can provide complementary information to pions:

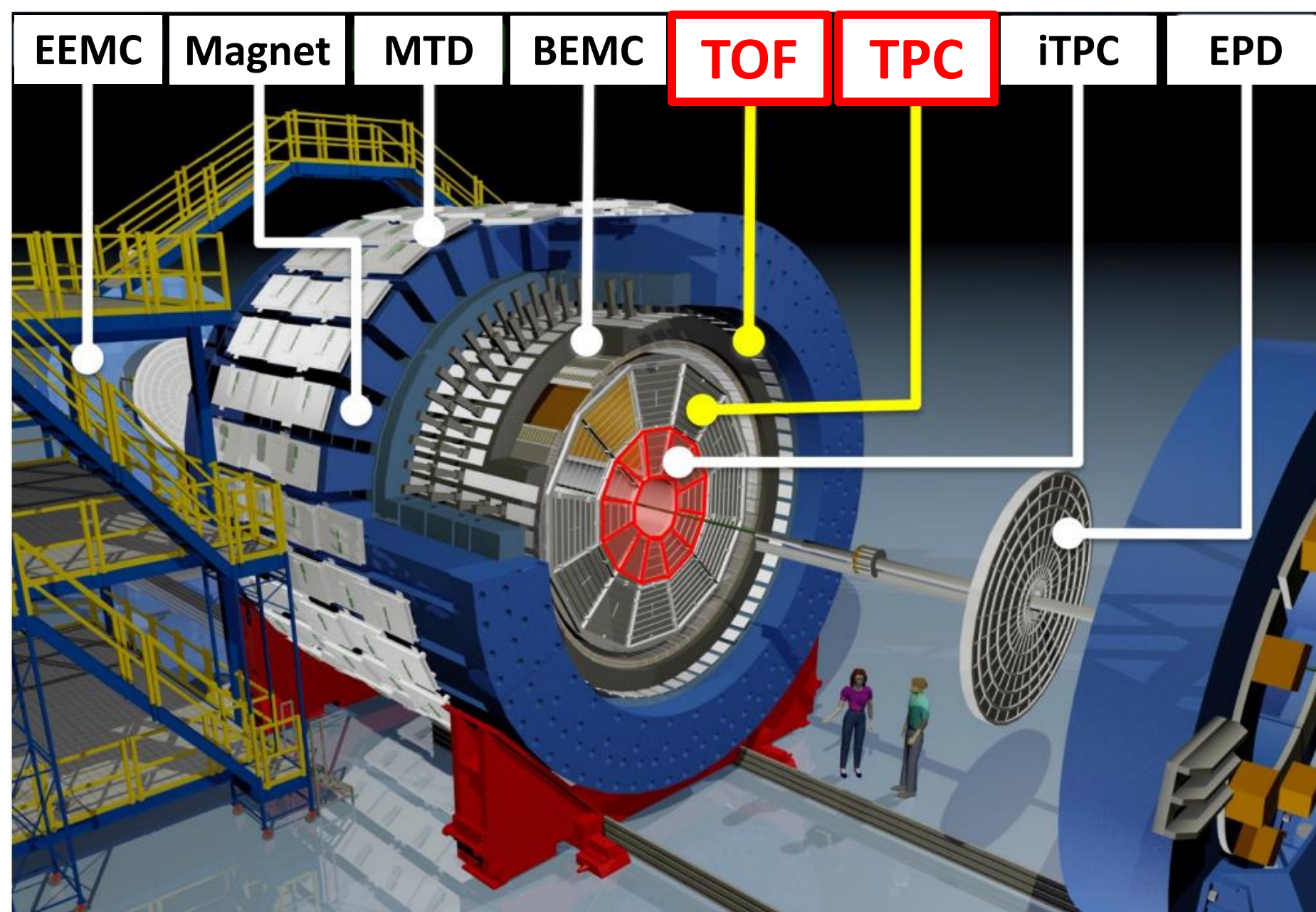
- contain strange quarks (larger production of strange particles is one of the signatures of QGP)
- less affected by the feed-down from resonance decays
- smaller cross section on reaction with the hadronic matter

Very interesting:

- compare femtoscopic results for all possible kaon combination ($K^\pm K^\pm$, $K_S^0K_S^0$, $K_S^0K^\pm$)
- $K_S^0K^\pm$ - a_0 could be a 4-quark state (a tetraquark)



The STAR experiment



- Excellent particle identification
- Large, uniform acceptance at mid-rapidity

Time Projection Chamber

PID: dE/dx

Tracking

$$0 < \phi < 2\pi, |\eta| < 1$$

Time-Of-Flight

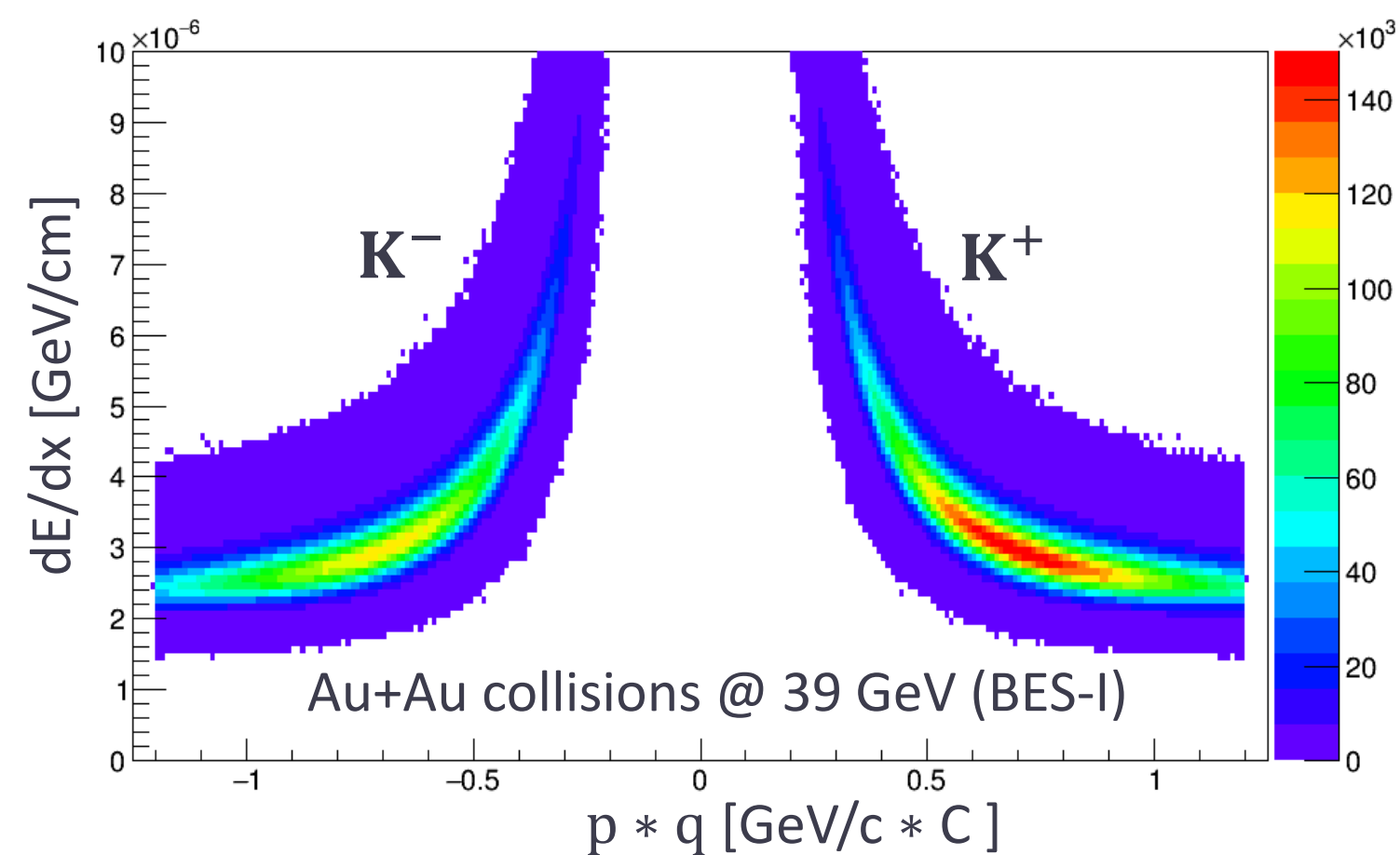
Time resolution < 80 ps

PID: m^2

Datasets

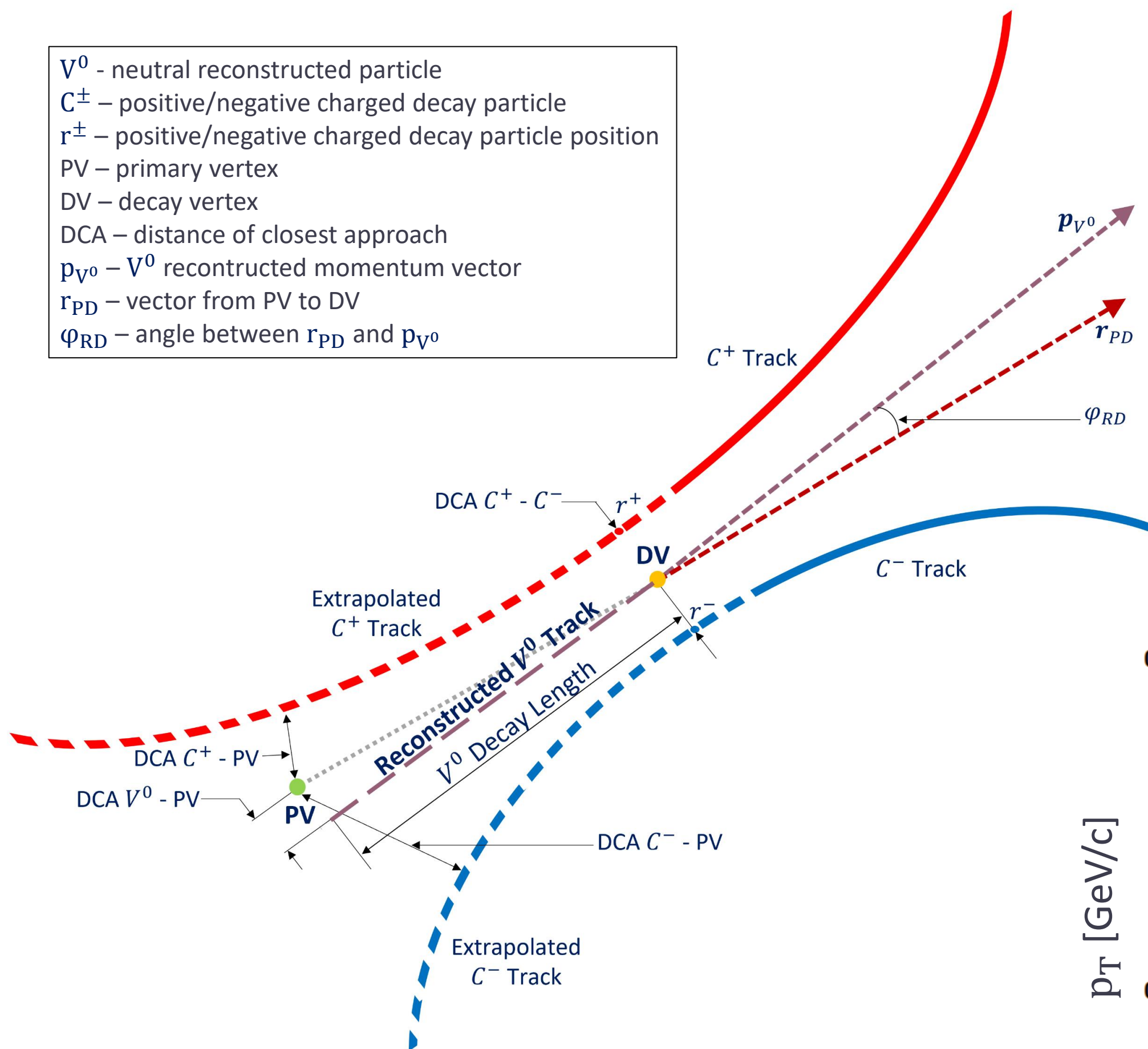
Energy $\sqrt{s_{NN}}$	Year	Mode	Statistics (M)
39 GeV	2010	Collider	~ 83
200 GeV	2010	Collider	~ 260

Au+Au collisions



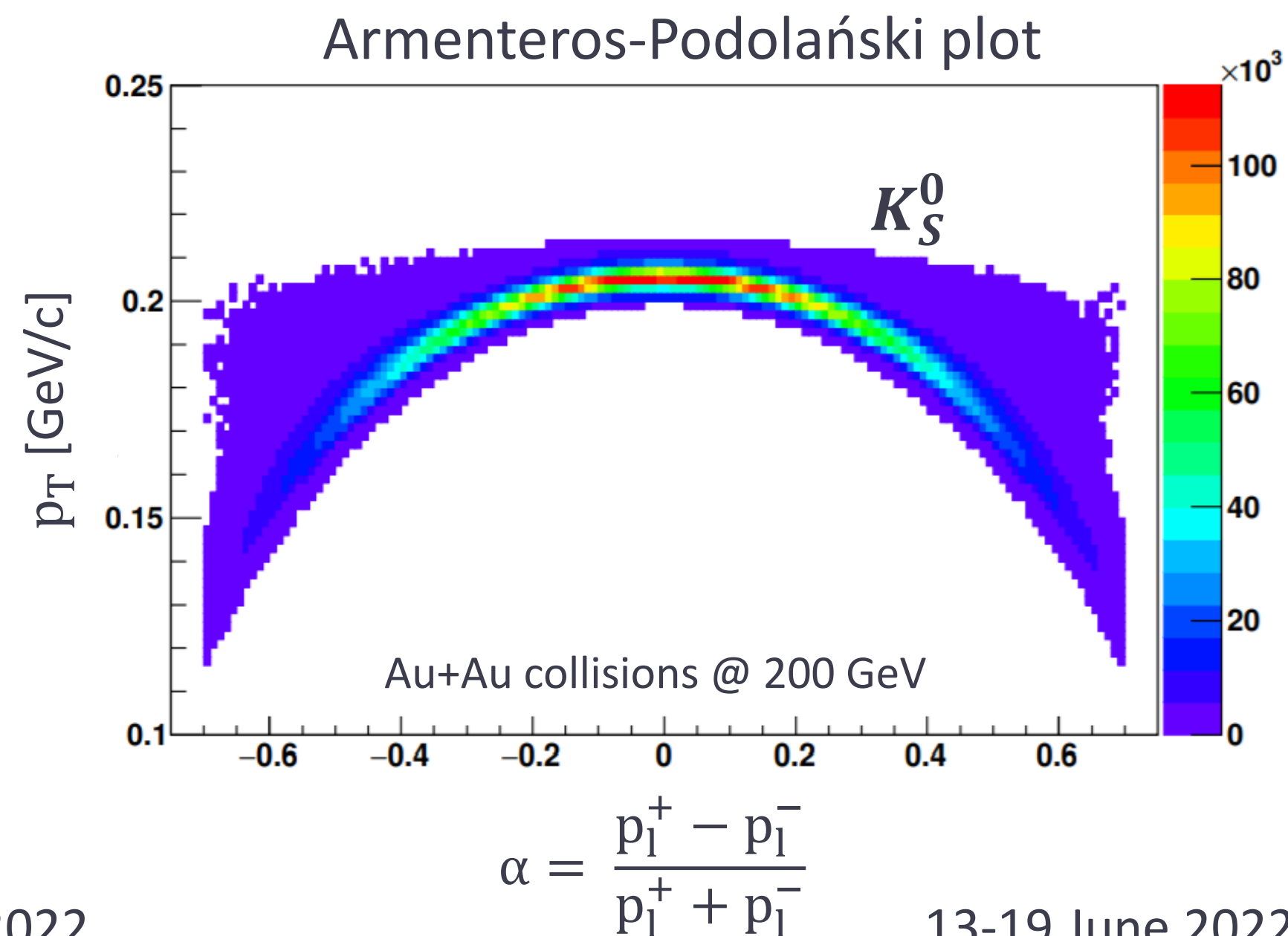
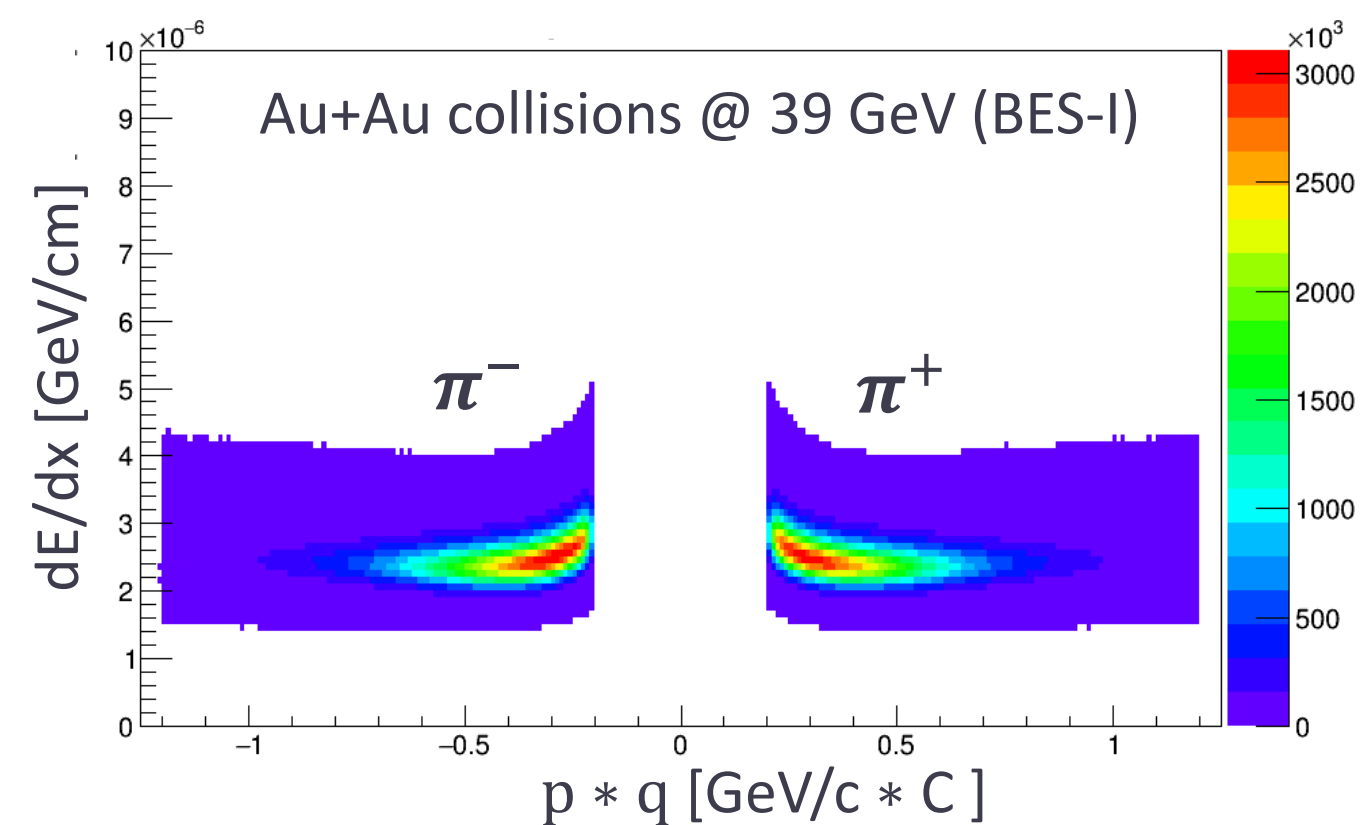
Neutral kaon reconstruction

V^0 - neutral reconstructed particle
 C^\pm - positive/negative charged decay particle
 r^\pm - positive/negative charged decay particle position
 PV - primary vertex
 DV - decay vertex
 DCA - distance of closest approach
 p_{V^0} - V^0 reconstructed momentum vector
 r_{PD} - vector from PV to DV
 φ_{RD} - angle between r_{PD} and p_{V^0}



$$K_S^0 \rightarrow \pi^+ \pi^- (69.20 \pm 0.05)\%$$

$$K_S^0 \rightarrow \pi^0 \pi^0 (30.69 \pm 0.05)\%$$



Parametrization - $K_S^0 K_S^0$

Gaussian density distribution (includes only QS effects): $CF(q_{inv}) = 1 + \lambda e^{-R_{inv}^2 q_{inv}^2}$

λ - the correlation strength, R_{inv} - the size of the particle-emitting source.

Lednicky & Lyuboshitz model includes **strong FSI**: [Sov.J.Nucl.Phys. 35, 770 (1982)]

$$CF(q_{inv}) = 1 + \lambda \left(e^{-R_{inv}^2 q_{inv}^2} + \frac{1}{2} \left[\left| \frac{f(k^*)}{R_{inv}} \right|^2 + \frac{4\Re f(k^*)}{\sqrt{\pi} R_{inv}} F_1(q_{inv} R_{inv}) - \frac{2\Im f(k^*)}{\sqrt{\pi} R_{inv}} F_2(q_{inv} R_{inv}) \right] \right)$$



Parametrization - $K_S^0 K_S^0$

Gaussian density distribution (includes only **QS effects**): $CF(q_{inv}) = 1 + \lambda e^{-R_{inv}^2 q_{inv}^2}$

λ - the correlation strength, R_{inv} - the size of the particle-emitting source.

Lednicky & Lyuboshitz model includes **strong FSI**: [Sov.J.Nucl.Phys. 35, 770 (1982)]

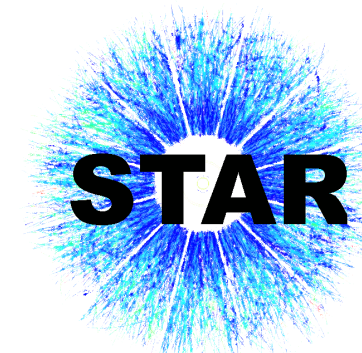
$$CF(q_{inv}) = 1 + \lambda \left(\underbrace{e^{-R_{inv}^2 q_{inv}^2}}_{\text{QS effect}} + \underbrace{\frac{1}{2} \left[\left| \frac{f(k^*)}{R_{inv}} \right|^2 + \frac{4\Re f(k^*)}{\sqrt{\pi} R_{inv}} F_1(q_{inv} R_{inv}) - \frac{2\Im f(k^*)}{\sqrt{\pi} R_{inv}} F_2(q_{inv} R_{inv}) \right]}_{\text{strong FSI through the } f_0(980) \text{ and } a_0(980) \text{ resonances}} \right)$$

QS effect

strong FSI through the $f_0(980)$ and $a_0(980)$ resonances

$$F_1(z) = \int_0^z dx \frac{e^{x^2} - x^2}{z}, \quad F_2(z) = \frac{1 - e^{x^2}}{z}$$

$$f(k^*) = \frac{1}{2} [f_0(k^*) + f_1(k^*)], \quad f_I(k^*) = \frac{\gamma_r}{m_r - s - i\gamma_r k^* - i\gamma_r' k_r'}, \quad s = 4(m_K^2 + k^{*2})$$



Parametrization - $K_S^0 K_S^0$

Gaussian density distribution (includes only QS effects): $CF(q_{inv}) = 1 + \lambda e^{-R_{inv}^2 q_{inv}^2}$

λ - the correlation strength, R_{inv} - the size of the particle-emitting source.

Lednicky & Lyuboshitz model includes **strong FSI**: [Sov.J.Nucl.Phys. 35, 770 (1982)]

$$CF(q_{inv}) = 1 + \lambda \left(\underbrace{e^{-R_{inv}^2 q_{inv}^2}}_{\text{QS effect}} + \underbrace{\frac{1}{2} \left[\left| \frac{f(k^*)}{R_{inv}} \right|^2 + \frac{4\Re f(k^*)}{\sqrt{\pi} R_{inv}} F_1(q_{inv} R_{inv}) - \frac{2\Im f(k^*)}{\sqrt{\pi} R_{inv}} F_2(q_{inv} R_{inv}) \right]}_{\text{strong FSI through the } f_0(980) \text{ and } a_0(980) \text{ resonances}} \right)$$

QS effect

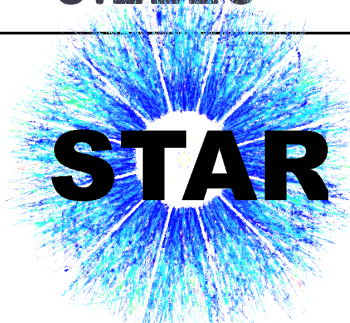
strong FSI through the $f_0(980)$ and $a_0(980)$ resonances

$$F_1(z) = \int_0^z dx \frac{e^{x^2} - x^2}{z}, \quad F_2(z) = \frac{1 - e^{z^2}}{z}$$

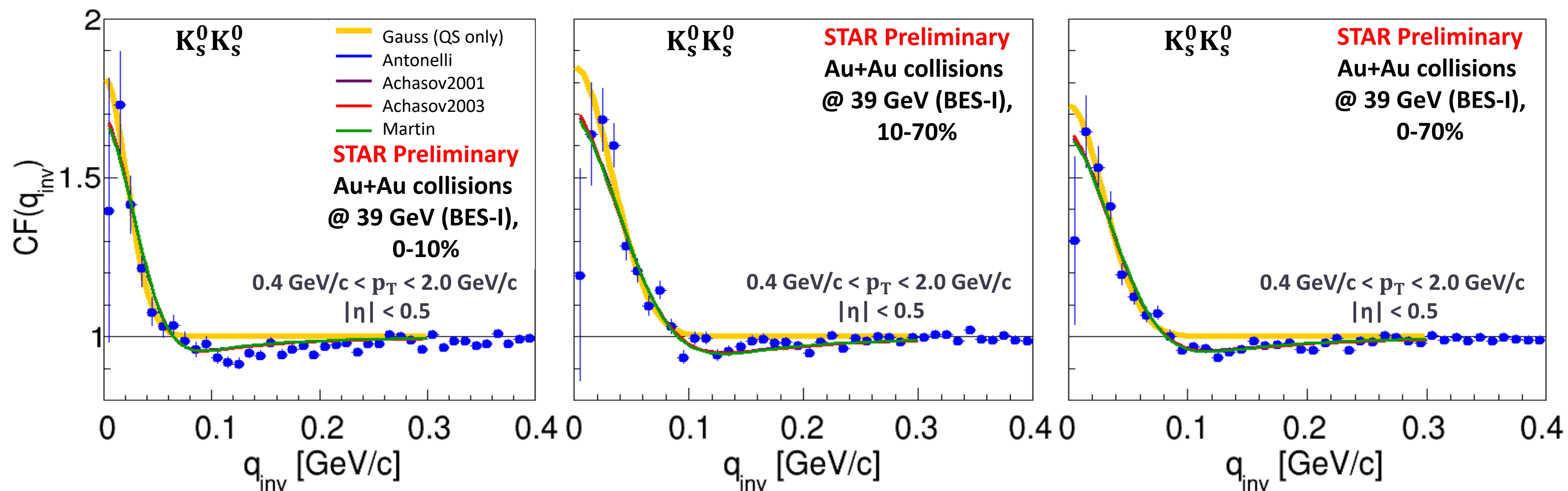
$$f(k^*) = \frac{1}{2} [f_0(k^*) + f_1(k^*)], \quad f_I(k^*) = \frac{\gamma_r}{m_r - s - i\gamma_r k^* - i\gamma_r' k_r'}, \quad s = 4(m_K^2 + k^{*2})$$

	$m_{f_0} \left[\frac{GeV}{c^2} \right]$	$\gamma_{f_0 K\bar{K}}$	$\gamma_{f_0 \pi\pi}$	$m_{a_0} \left[\frac{GeV}{c^2} \right]$	$\gamma_{a_0 K\bar{K}}$	$\gamma_{a_0 \pi\pi}$
Antonelli [1]	0.973	2.763	0.5283	0.985	0.4038	0.3711
Achasov2001 [2]	0.996	1.305	0.2684	0.992	0.5555	0.4401
Achasov2003 [3]	0.996	1.305	0.2684	1.003	0.8365	0.4580
Martin [4]	0.978	0.792	0.1990	0.974	0.3330	0.2220

[1] eConf C020620, THAT06 (2002), [2] Phys. Rev. D 63, 094007 (2001)
 [3] Phys. Rev. D 68, 014006 (2003), [4] Nucl. Phys. B 121, 514–530 (1977)



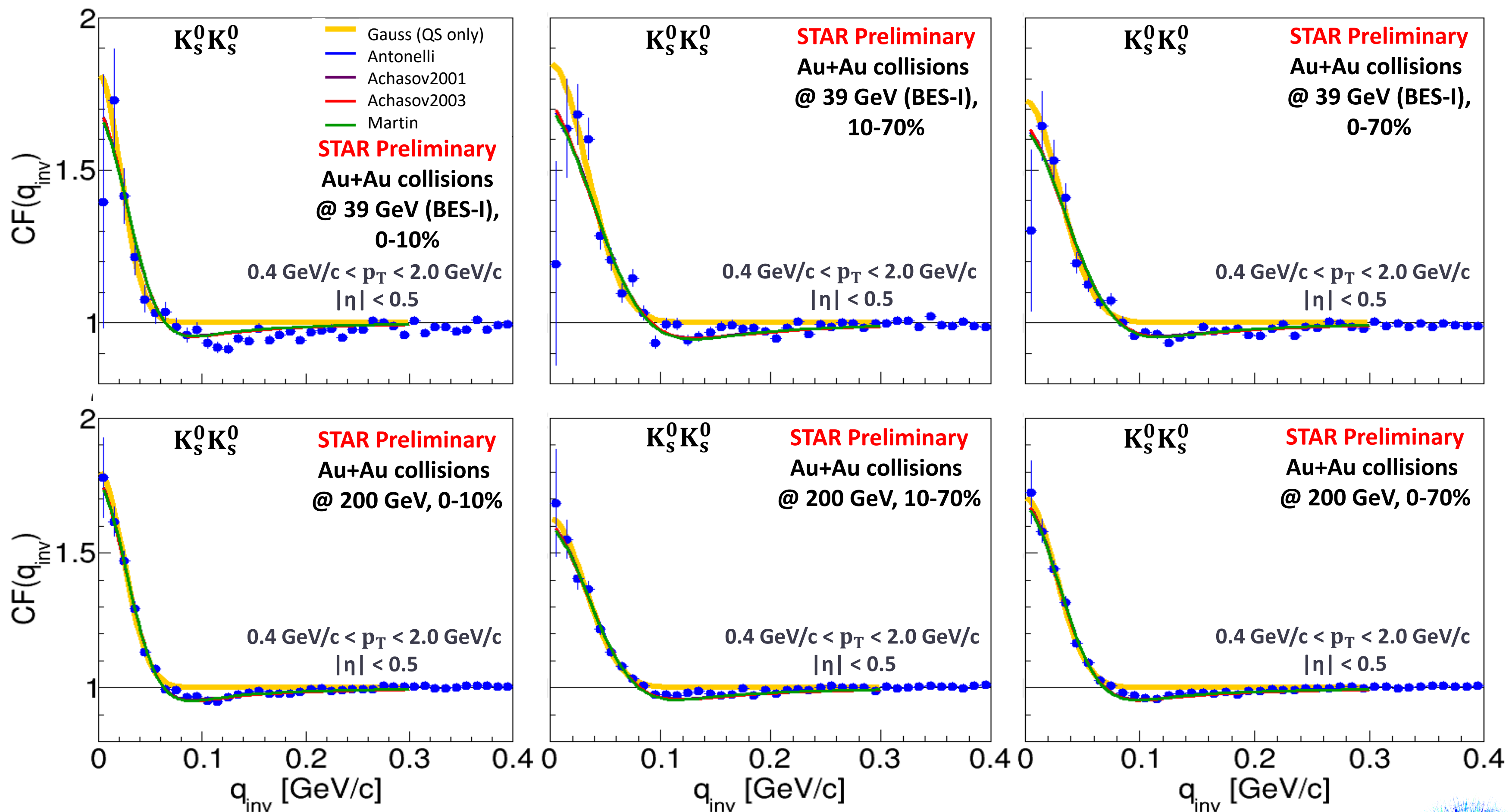
$K_S^0 K_S^0$ femtoscopy at 39 GeV & 200 GeV



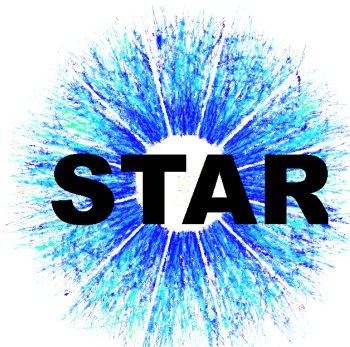
$$q_{inv} = \sqrt{(\vec{p}_1 - \vec{p}_2)^2 - (E_1 - E_2)^2}$$



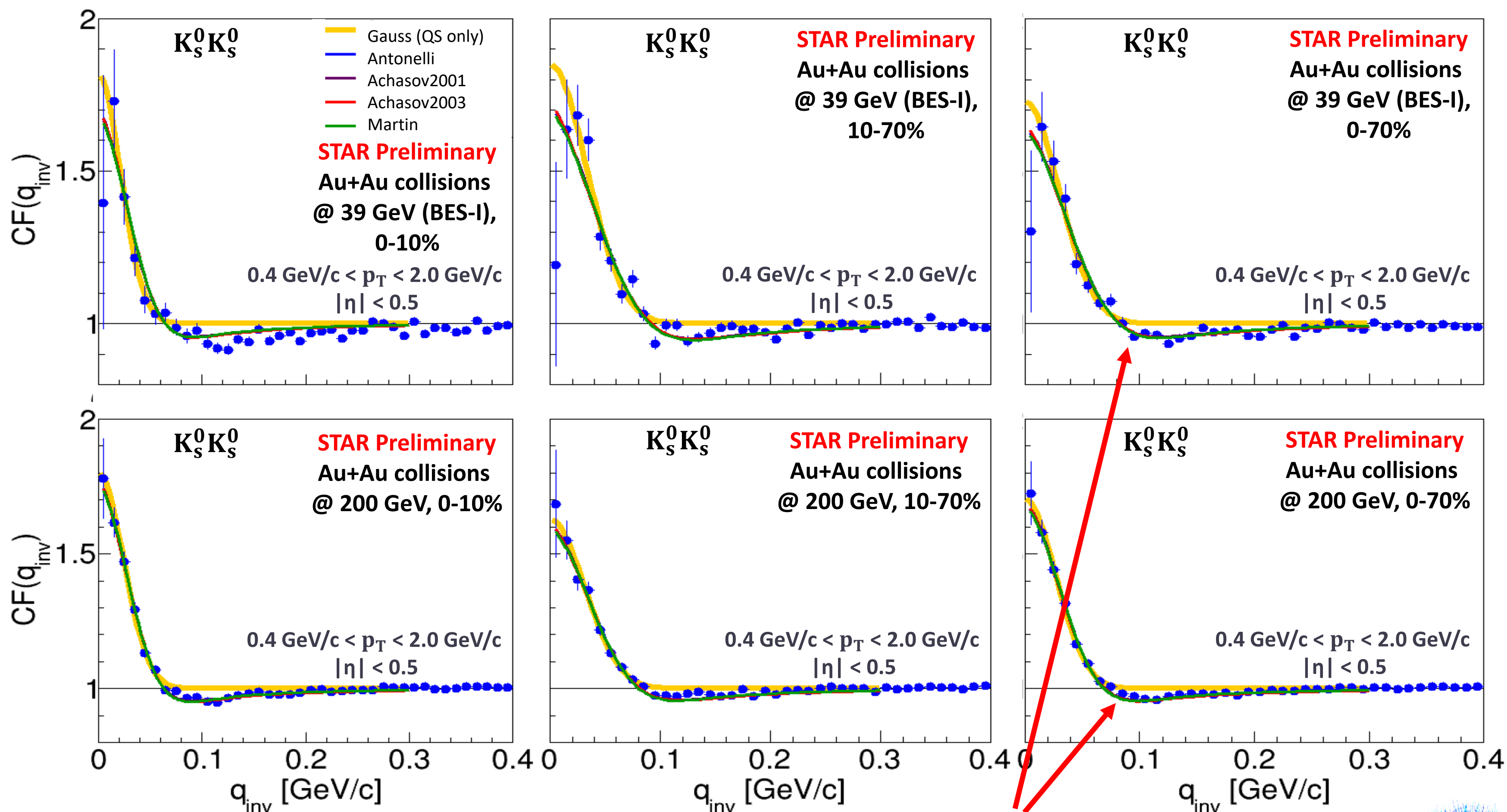
$K_S^0 K_S^0$ femtoscopy at 39 GeV & 200 GeV



$$q_{inv} = \sqrt{(\vec{p}_1 - \vec{p}_2)^2 - (E_1 - E_2)^2}$$

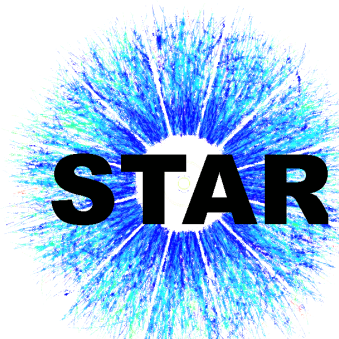


$K_S^0 K_S^0$ femtoscopy at 39 GeV & 200 GeV

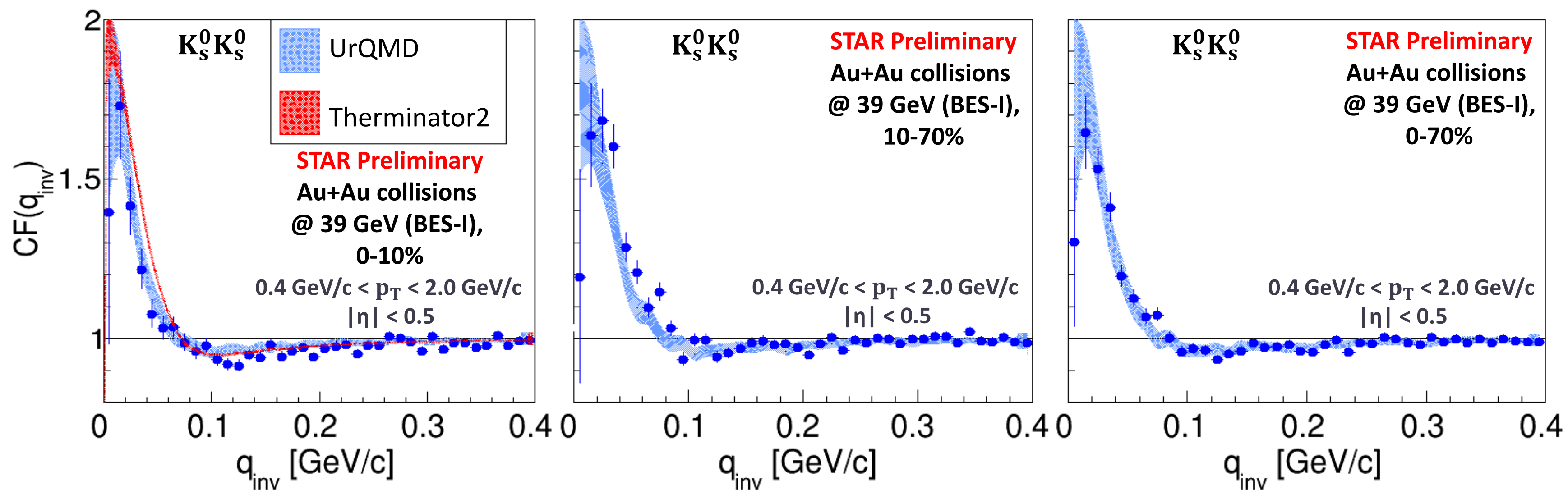


FSI is needed to reproduce the dip structure

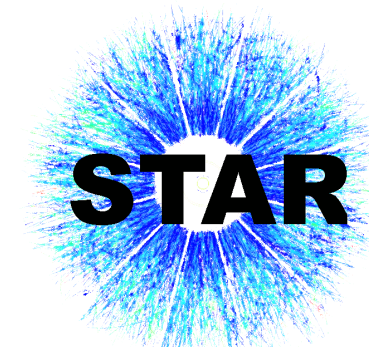
$$q_{inv} = \sqrt{(\vec{p}_1 - \vec{p}_2)^2 - (E_1 - E_2)^2}$$



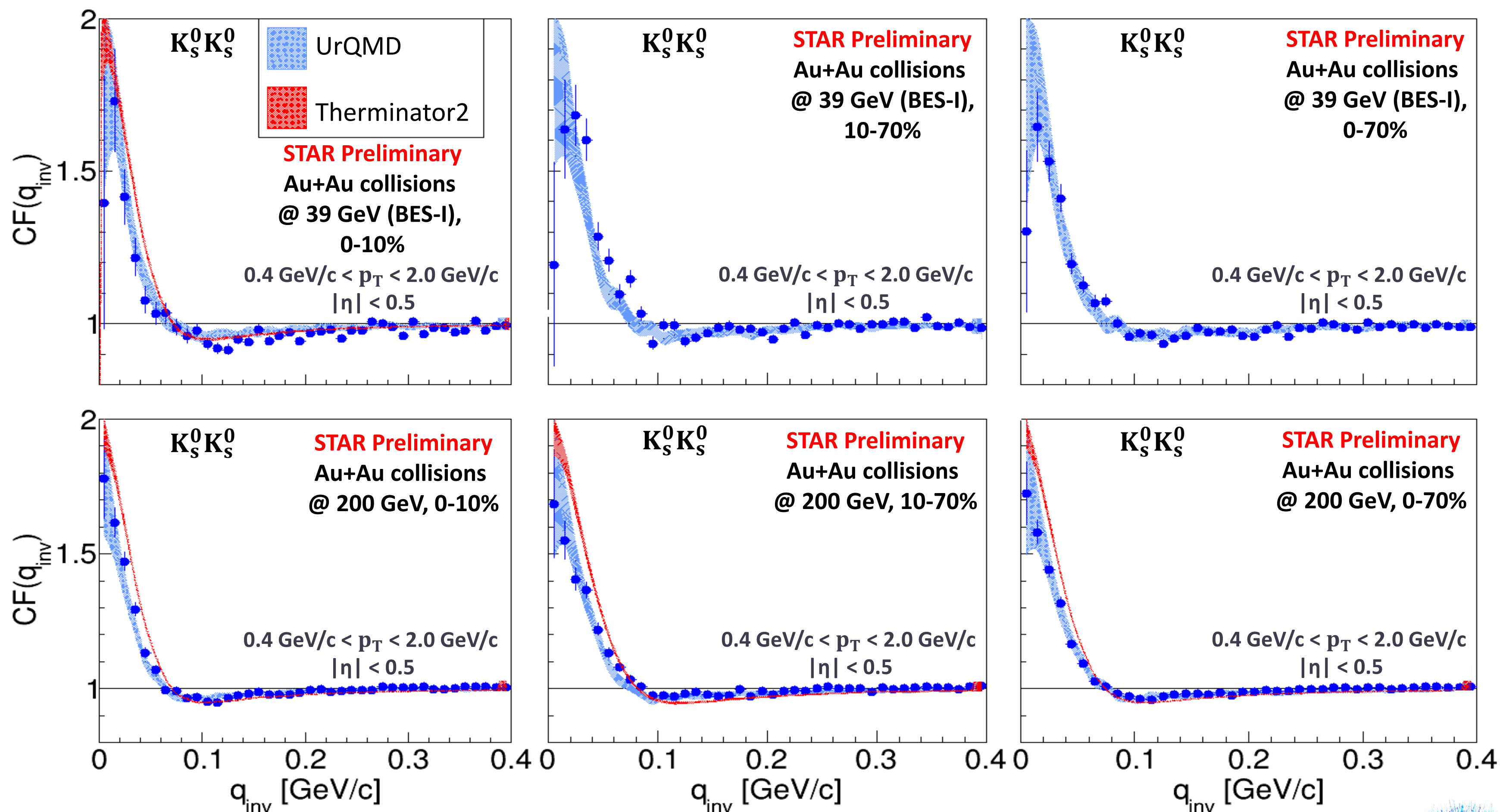
$K_S^0 K_S^0$ femtoscopy at 39 GeV & 200 GeV



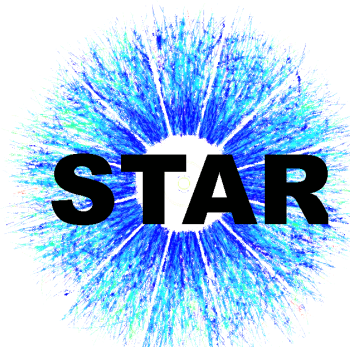
$$q_{inv} = \sqrt{(\vec{p}_1 - \vec{p}_2)^2 - (E_1 - E_2)^2}$$



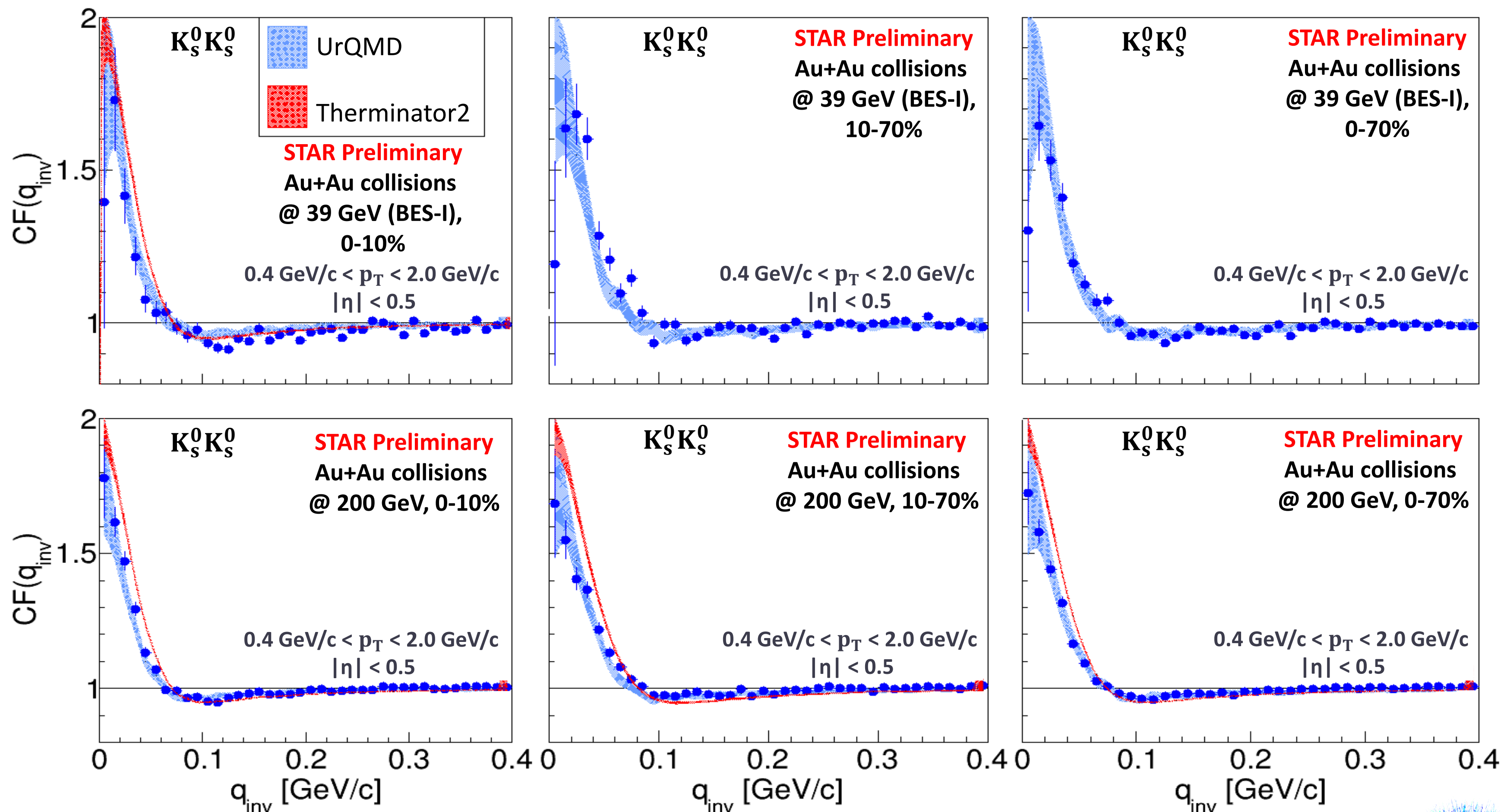
$K_S^0 K_S^0$ femtoscopy at 39 GeV & 200 GeV



$$q_{inv} = \sqrt{(\vec{p}_1 - \vec{p}_2)^2 - (E_1 - E_2)^2}$$



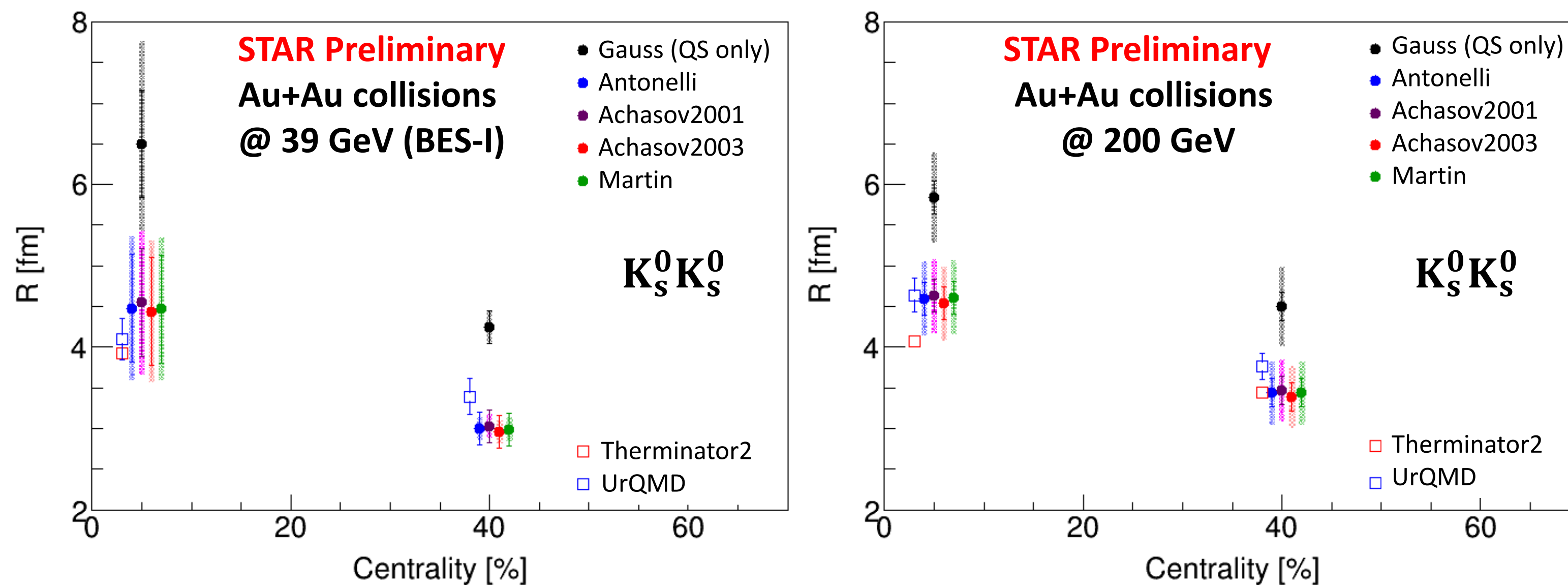
$K_S^0 K_S^0$ femtoscopy at 39 GeV & 200 GeV



Good agreement of the experimental points with the models

$$q_{inv} = \sqrt{(\vec{p}_1 - \vec{p}_2)^2 - (E_1 - E_2)^2}$$

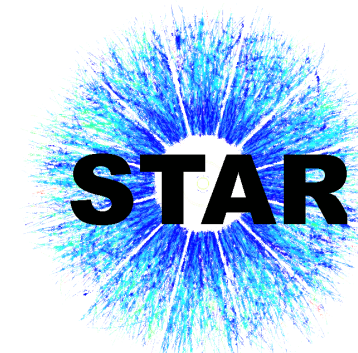
$K_S^0 K_S^0$ femtoscopy – centrality dependence



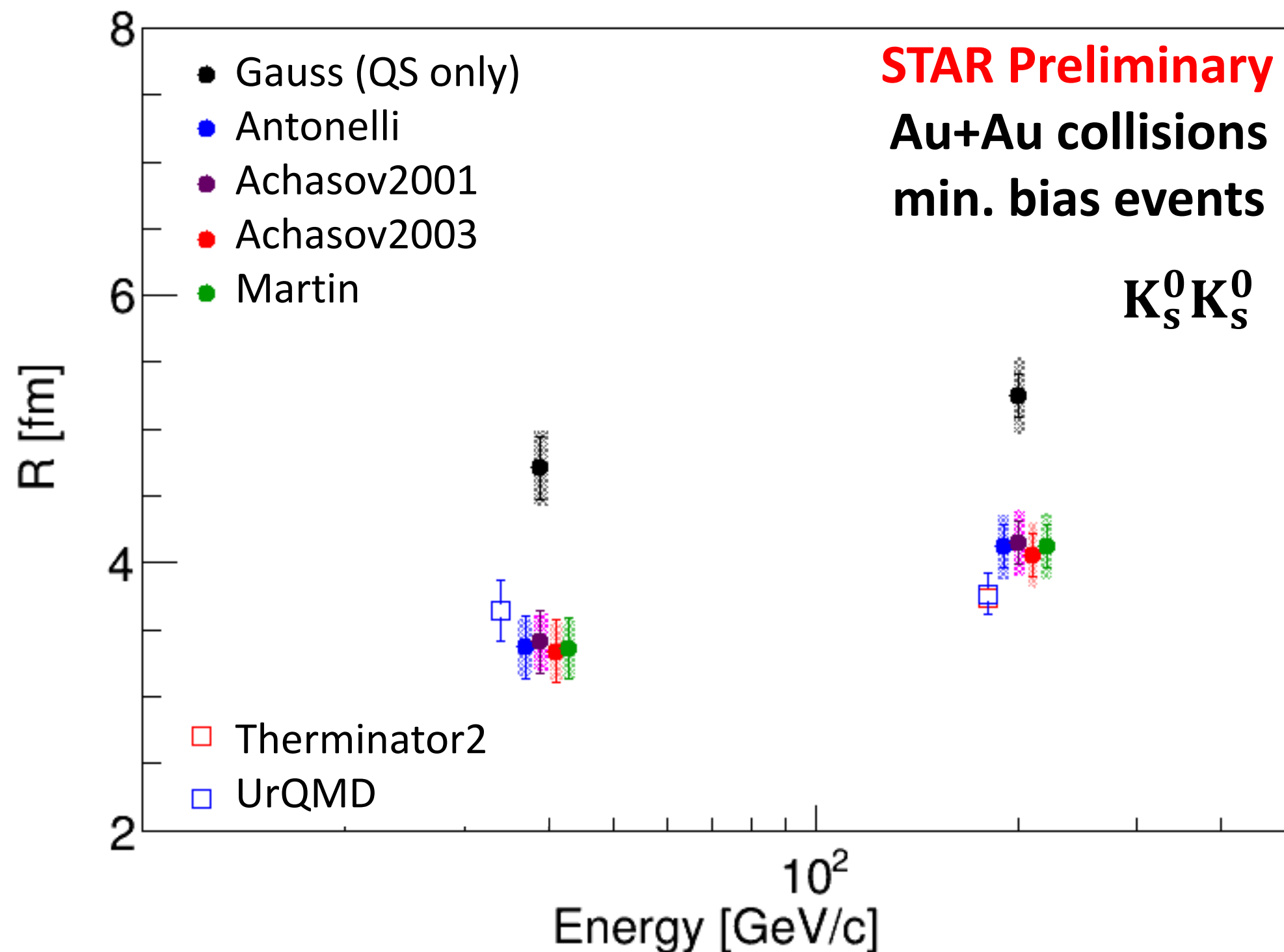
- Visible centrality dependence

$$R_{0-10\%} > R_{10-70\%}$$

- Only Gaussian assumption leads to larger R , showing importance to include SI



$K_S^0 K_S^0$ femtoscopy – energy dependence



- Visible energy dependence for both parametrization
 $R_{200 \text{ GeV}} > R_{39 \text{ GeV}}$
- Source sizes from models and FSI parametrizations consistent within the range of uncertainty



Parametrization - $K_S^0 K^\pm$

Lednicky & Lyuboshitz model includes strong FSI: [Sov.J.Nucl.Phys. 35, 770 (1982)]

$$CF(k^*) = 1 + \frac{\lambda}{4} \left[\left| \frac{f(k^*)}{R} \right|^2 + \frac{4\Re f(k^*)}{\sqrt{\pi}R} F_1(2k^*R) - \frac{2\Im f(k^*)}{\sqrt{\pi}R} F_2(2k^*R) \right]$$



Parametrization - $K_S^0 K^\pm$

Lednicky & Lyuboshitz model includes strong FSI: [Sov.J.Nucl.Phys. 35, 770 (1982)]

$$CF(k^*) = 1 + \frac{\lambda}{4} \left[\left| \frac{f(k^*)}{R} \right|^2 + \frac{4\Re f(k^*)}{\sqrt{\pi}R} F_1(2k^*R) - \frac{2\Im f(k^*)}{\sqrt{\pi}R} F_2(2k^*R) \right]$$

strong FSI through the $a_0(980)$ resonance

$$F_1(z) = \int_0^z dx \frac{e^{x^2} - x^2}{z}, \quad F_2(z) = \frac{1 - e^{-z^2}}{z}$$

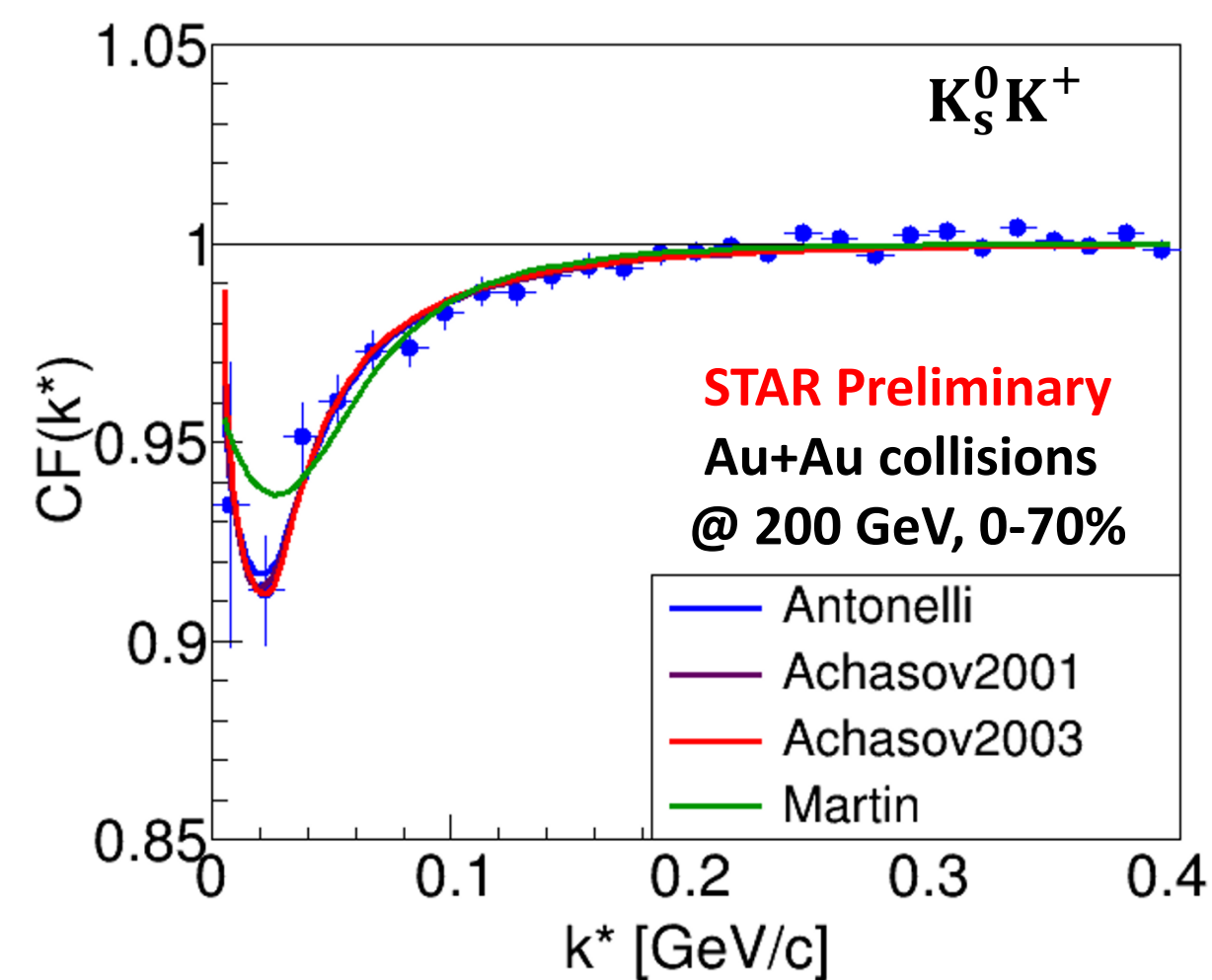
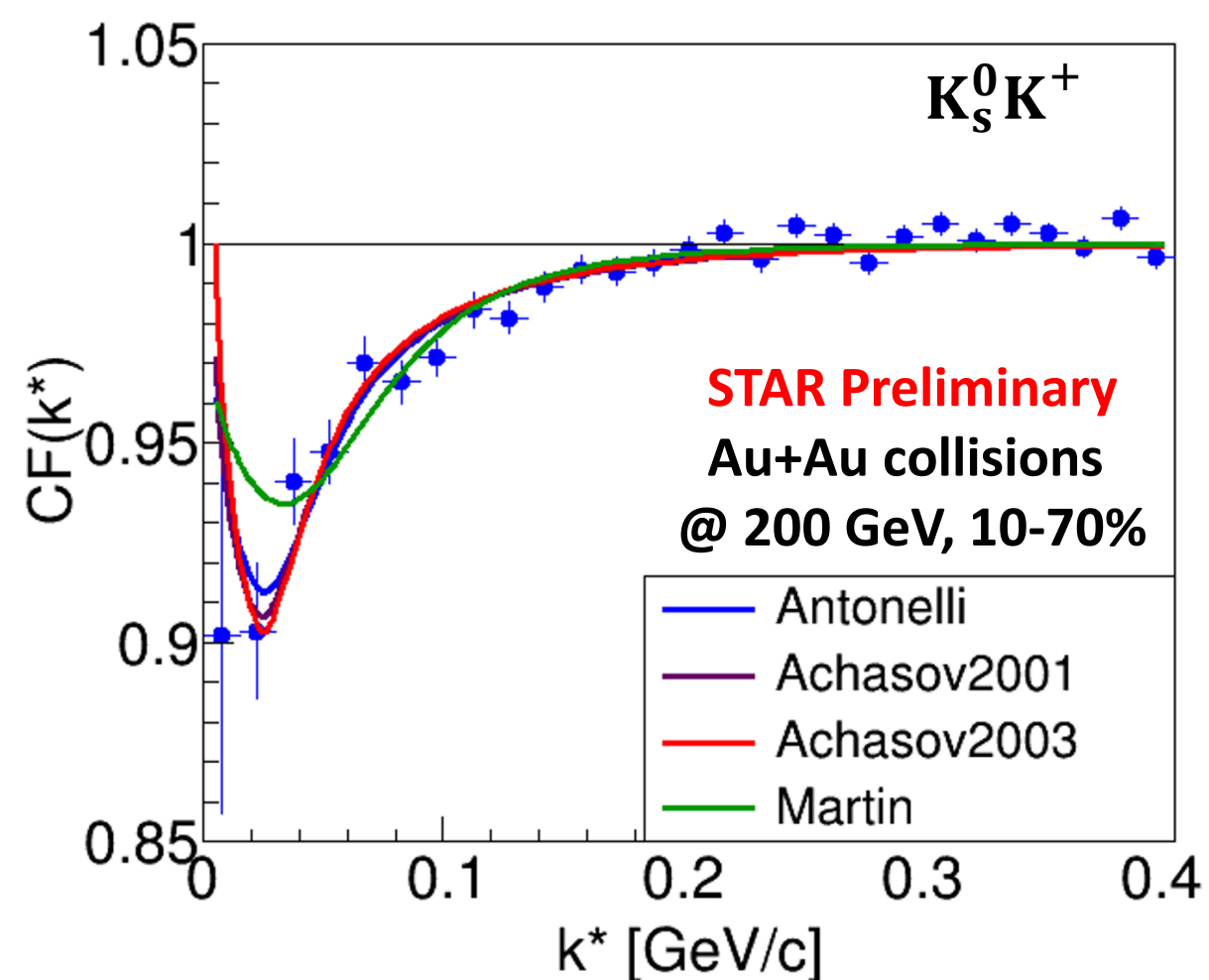
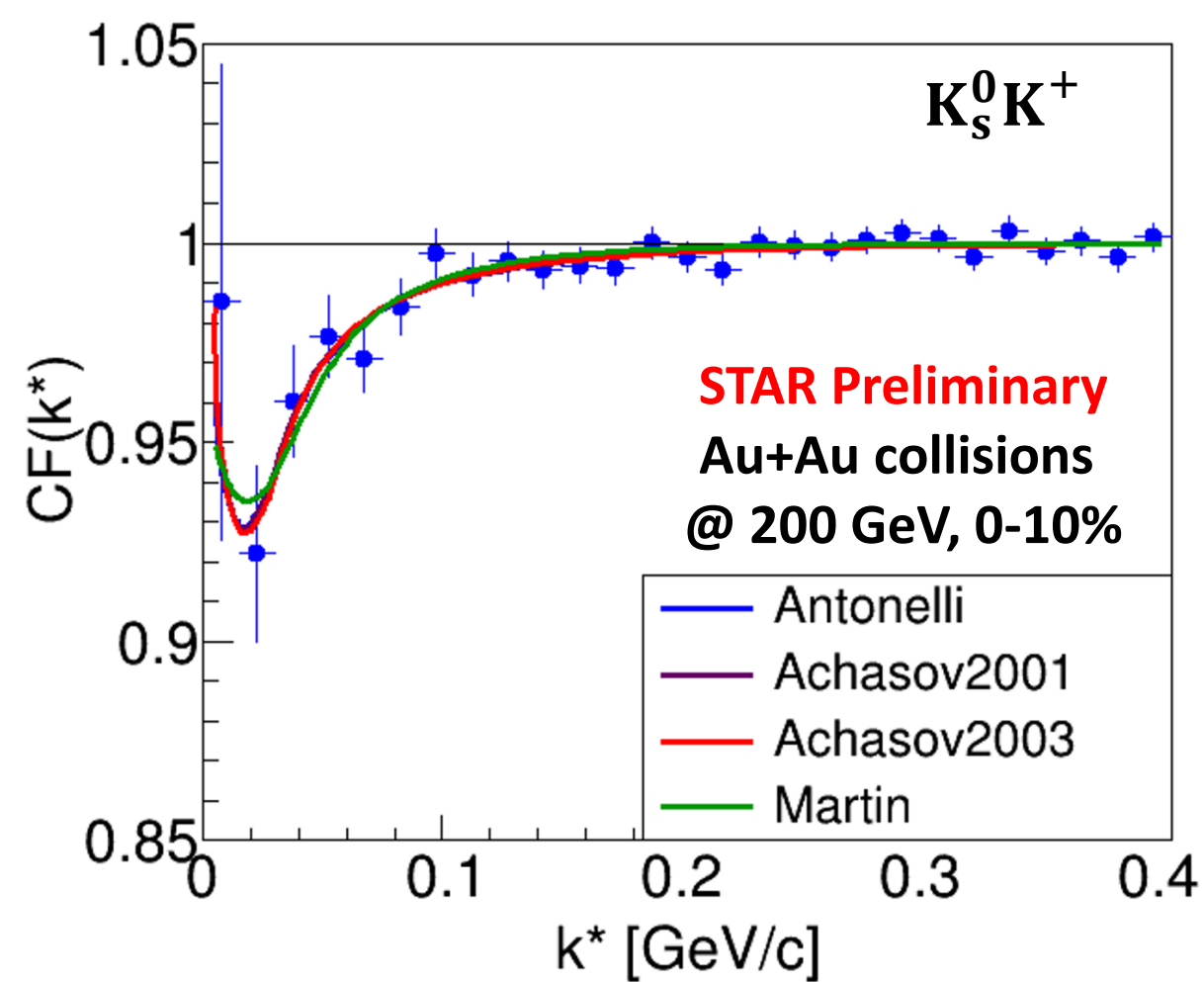
$$f(k^*) = \frac{\gamma_r}{m_r - s - i\gamma_r k^* - i\gamma_r' k_r'}, \quad s = 4(m_K^2 + k^{*2})$$

	$m_{a_0} \left[\frac{\text{GeV}}{c^2} \right]$	$\gamma_{a_0 K \bar{K}}$	$\gamma_{a_0 \pi \eta}$
Antonelli [1]	0.985	0.4038	0.3711
Achasov2001 [2]	0.992	0.5555	0.4401
Achasov2003 [3]	1.003	0.8365	0.4580
Martin [4]	0.974	0.3330	0.2220

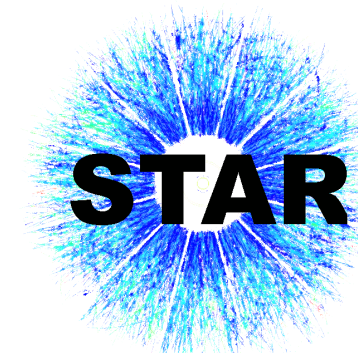
[1] eConf C020620, THAT06 (2002), [2] Phys. Rev. D 63, 094007 (2001)
 [3] Phys. Rev. D 68, 014006 (2003), [4] Nucl. Phys. B 121, 514–530 (1977)



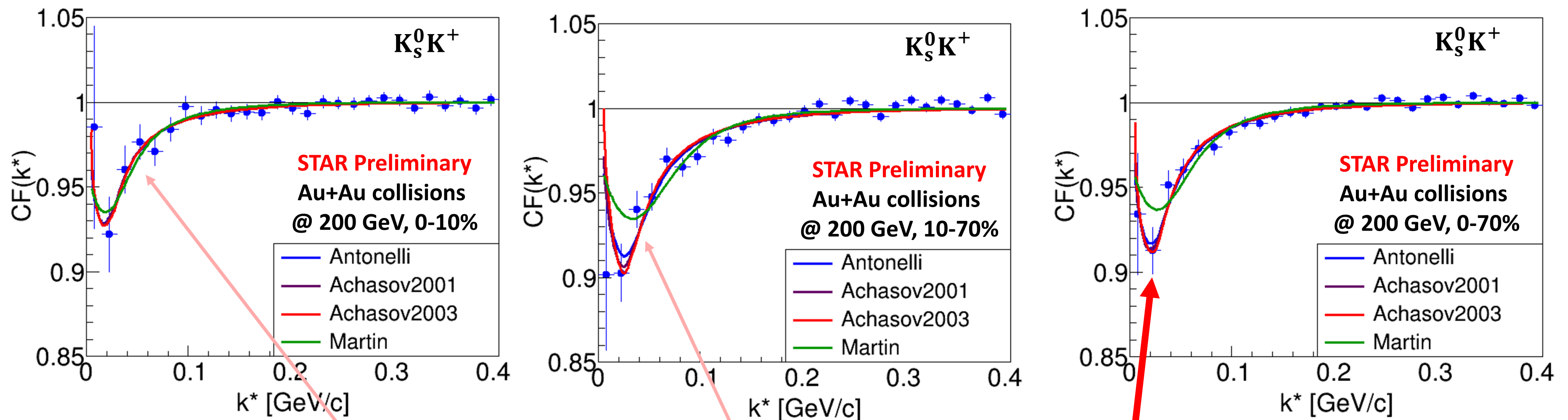
$K_S^0 K^+$ femtoscopy at 200 GeV



$$k^* = |\vec{p}_1| = |\vec{p}_2|$$



$K_S^0 K^+$ femtoscopy at 200 GeV

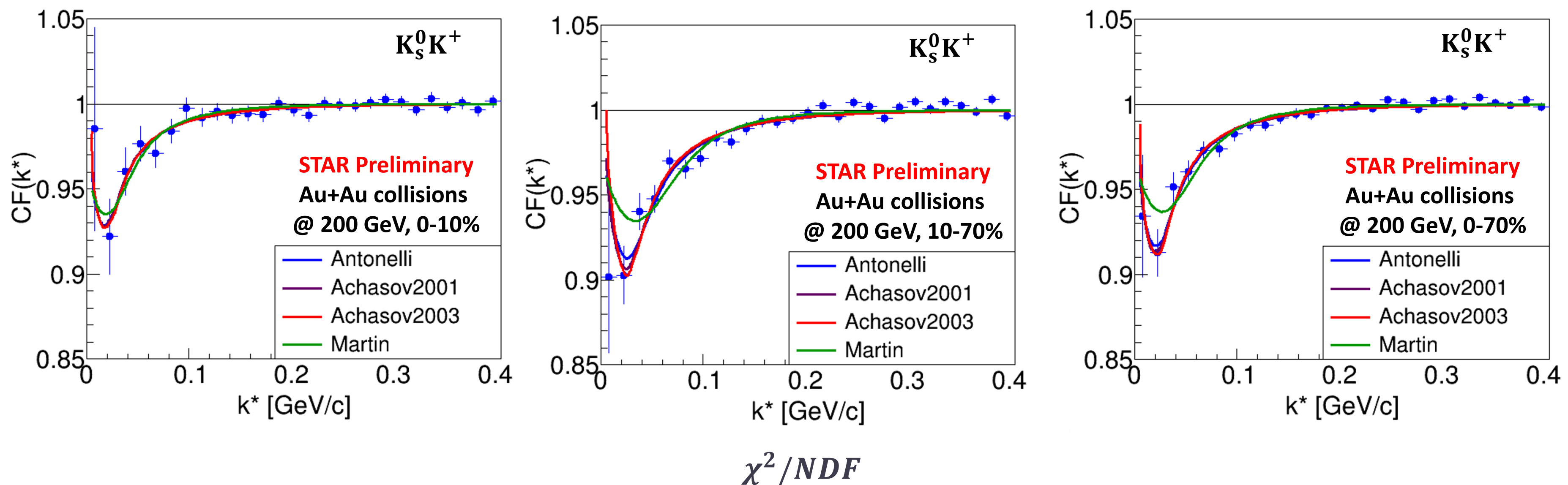


The a_0 FSI parametrization gives an excellent representation of the signal region of the data

$$k^* = |\vec{p}_1| = |\vec{p}_2| \quad \dots$$



$K_S^0 K^+$ femtoscopy at 200 GeV

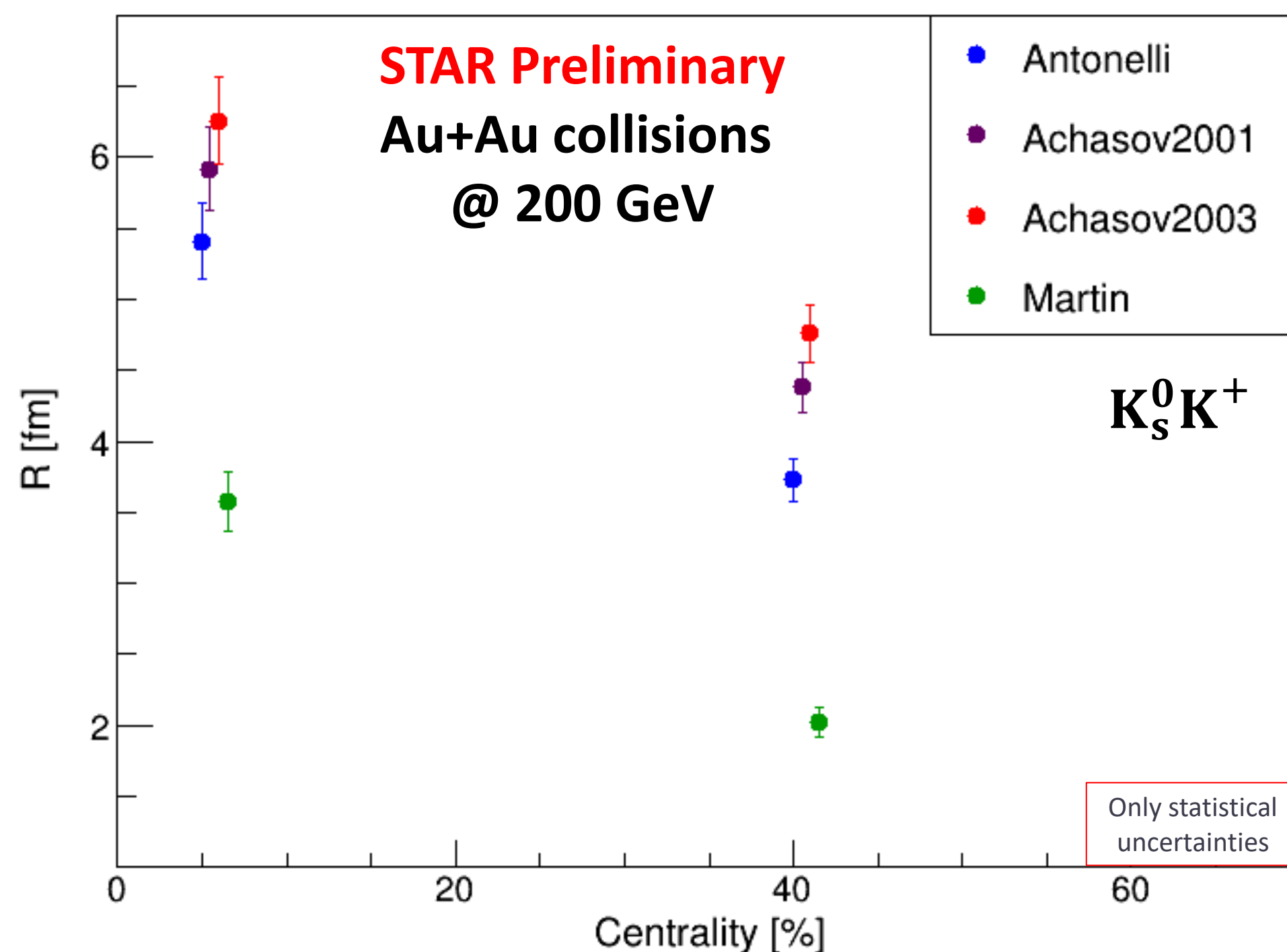


	0-10%	10-70%	0-70%
Antonelli [1]	0.60	1.66	1.04
Achasov2001 [2]	0.59	1.73	1.07
Achasov2003 [3]	0.58	1.85	1.14
Martin [4]	0.65	1.65	1.16

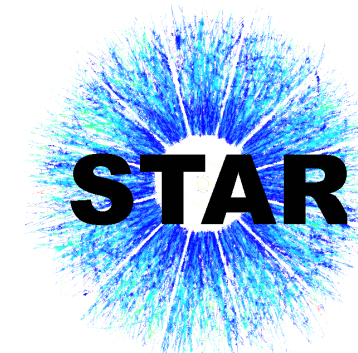
$$k^* = |\vec{p}_1| = |\vec{p}_2|$$



$K_S^0 K^+$ femtoscopy – centrality dependence



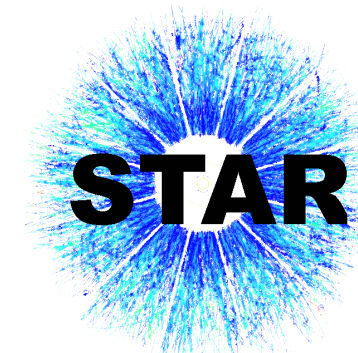
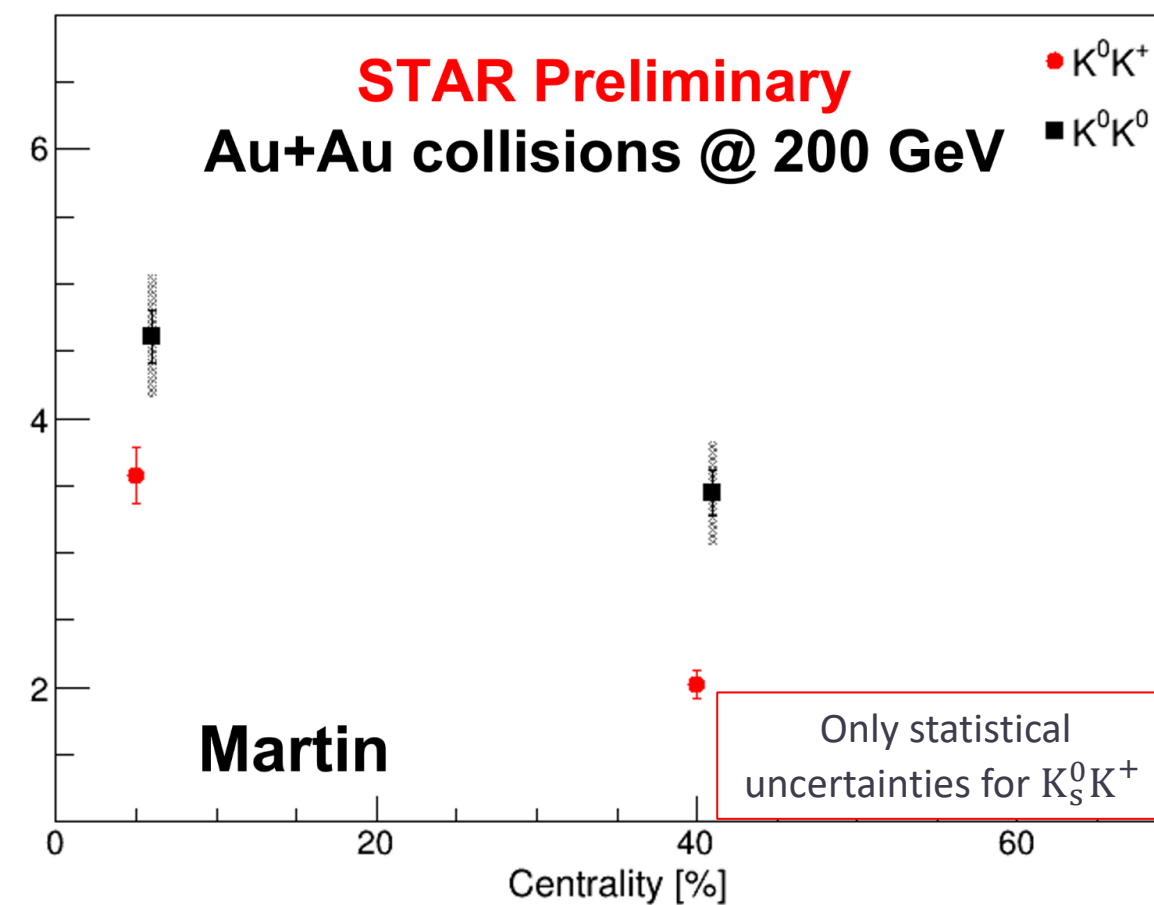
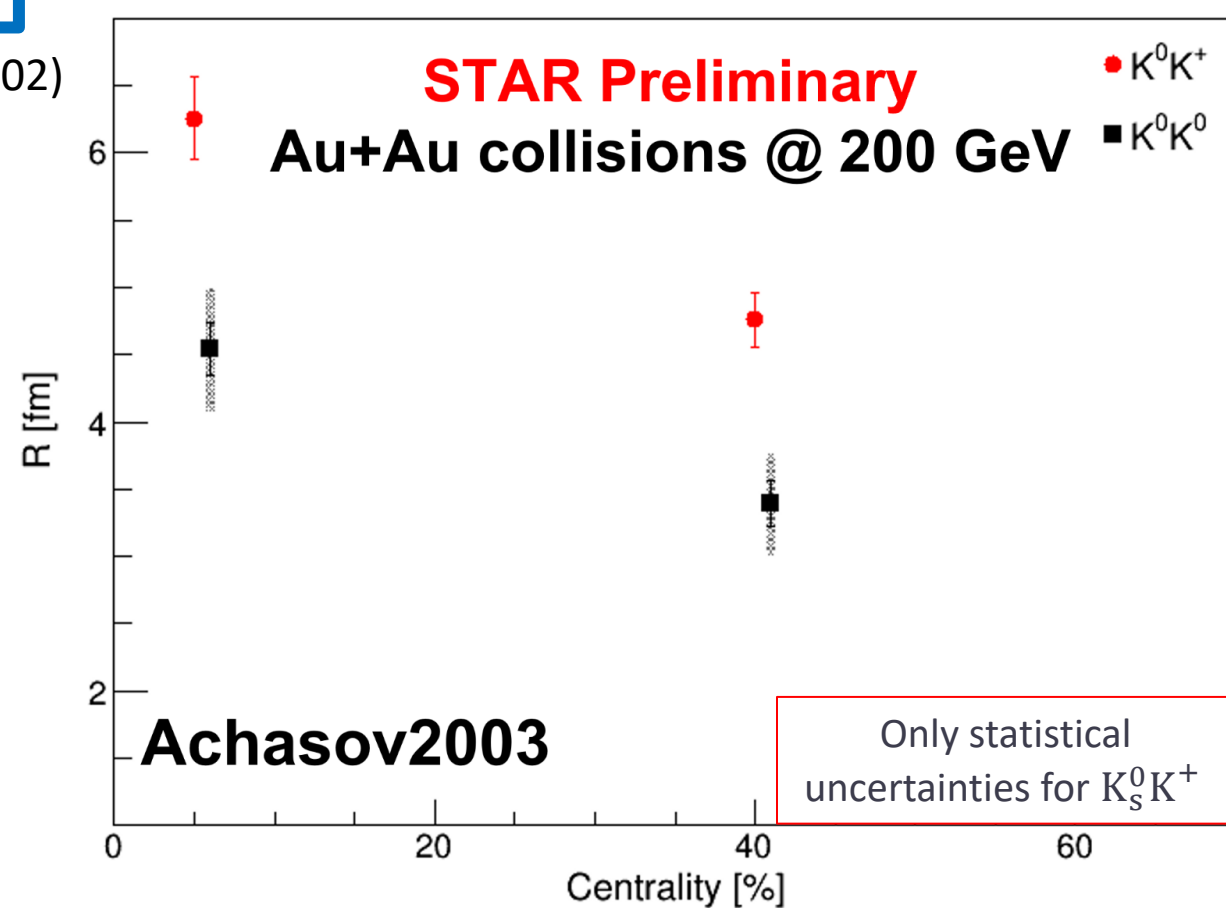
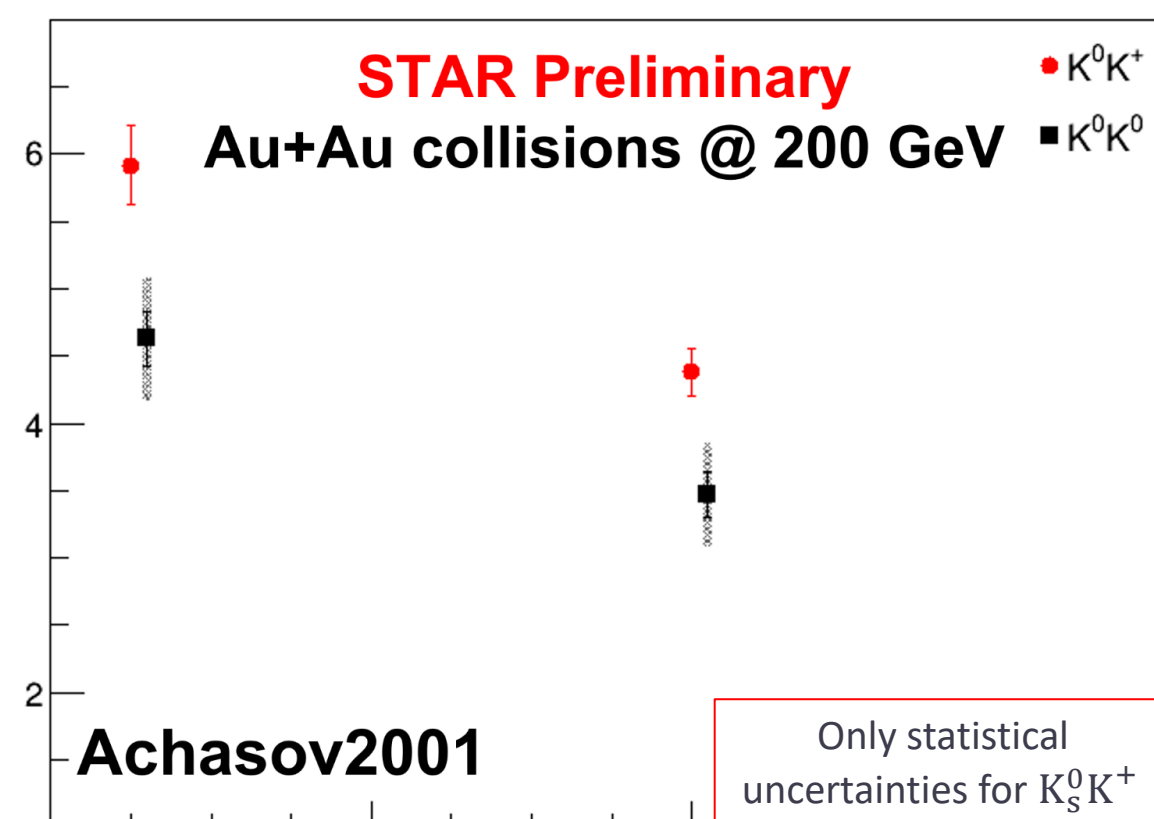
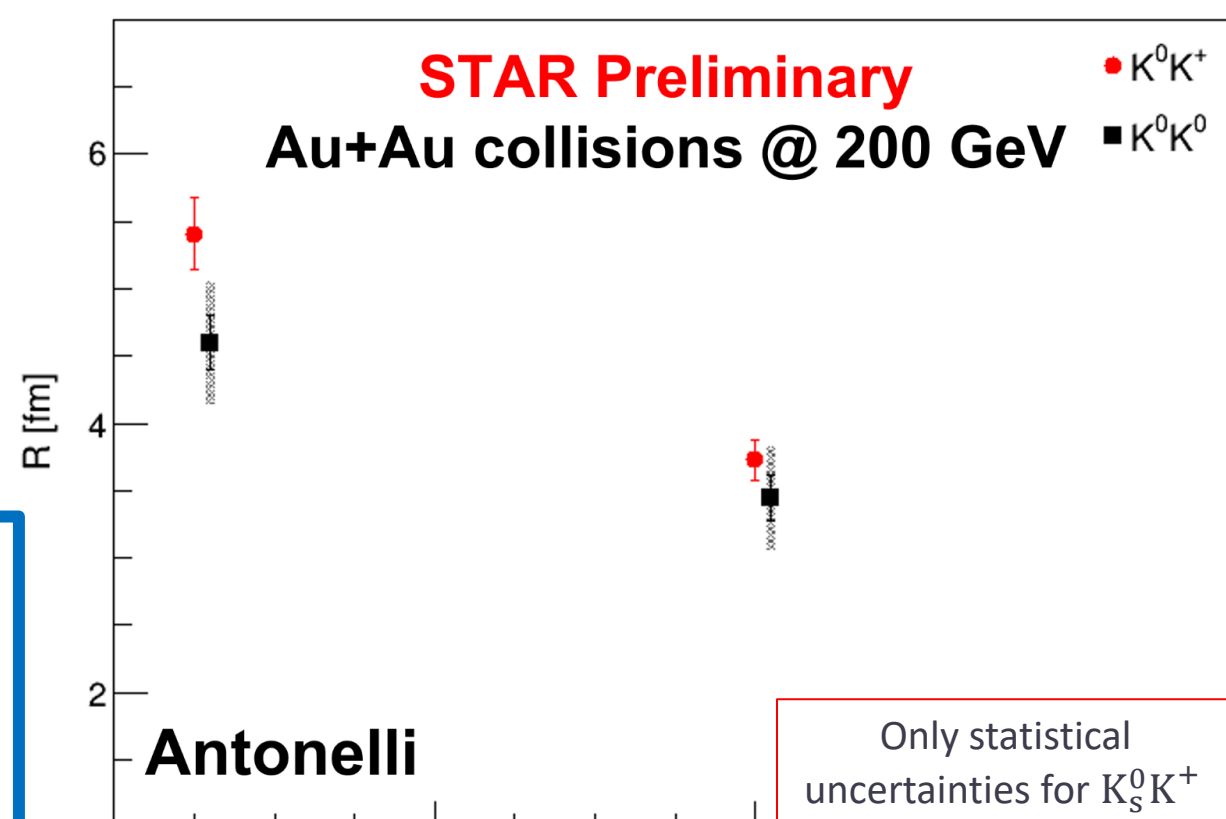
- Visible centrality dependence
 $R_{0-10\%} > R_{10-70\%}$
- Achasov2003** parametrization (the larger a_0 mass) gives the larger size of the source



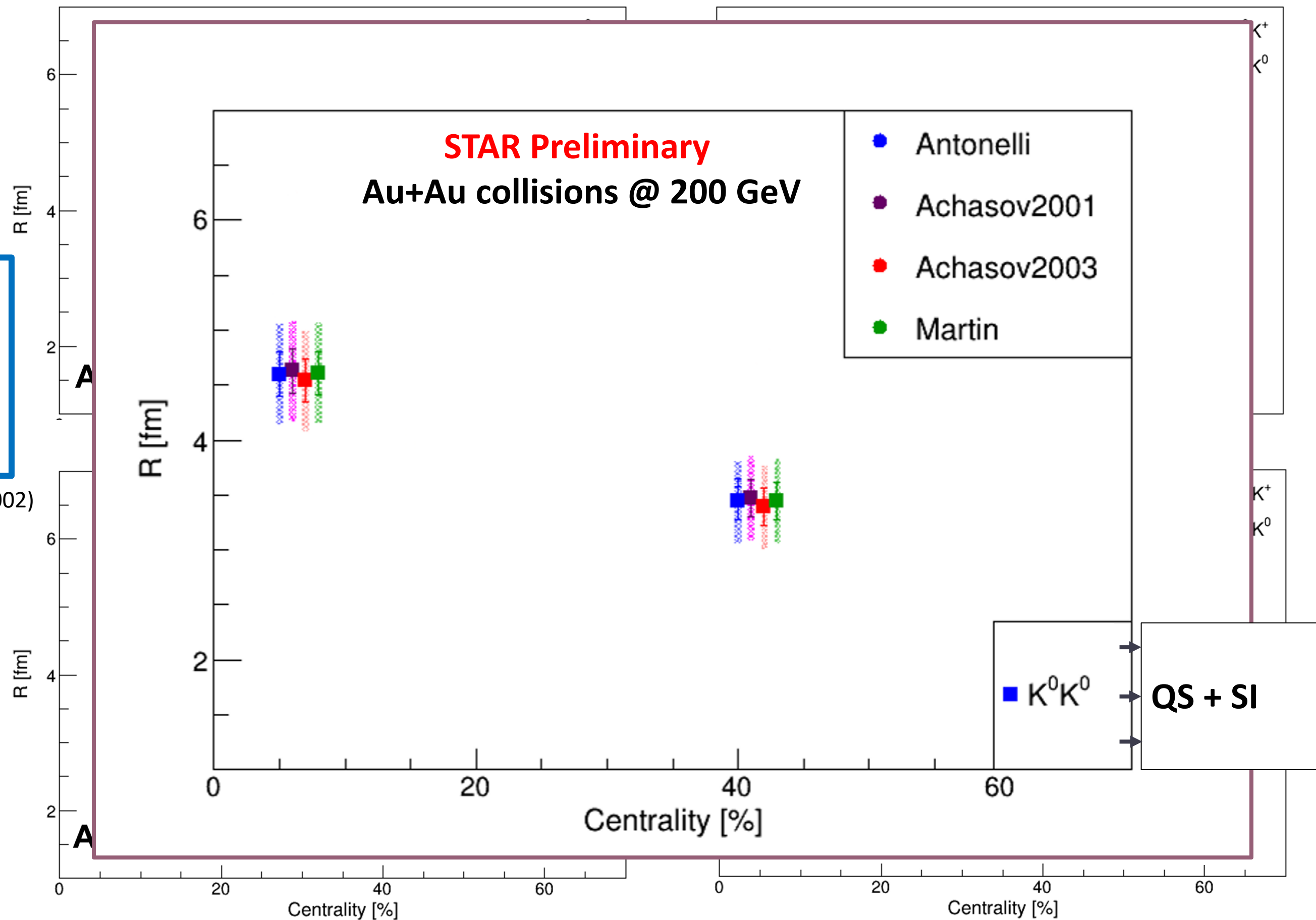
Comparison - $K_S^0 K_S^0$ and $K_S^0 K^+$ - 200 GeV

Antonelli
favors a_0
resonance as
a tetraquark

eConf C020620, THAT06 (2002)



Comparison - $K_S^0 K_S^0$ and $K_S^0 K^+$ - 200 GeV

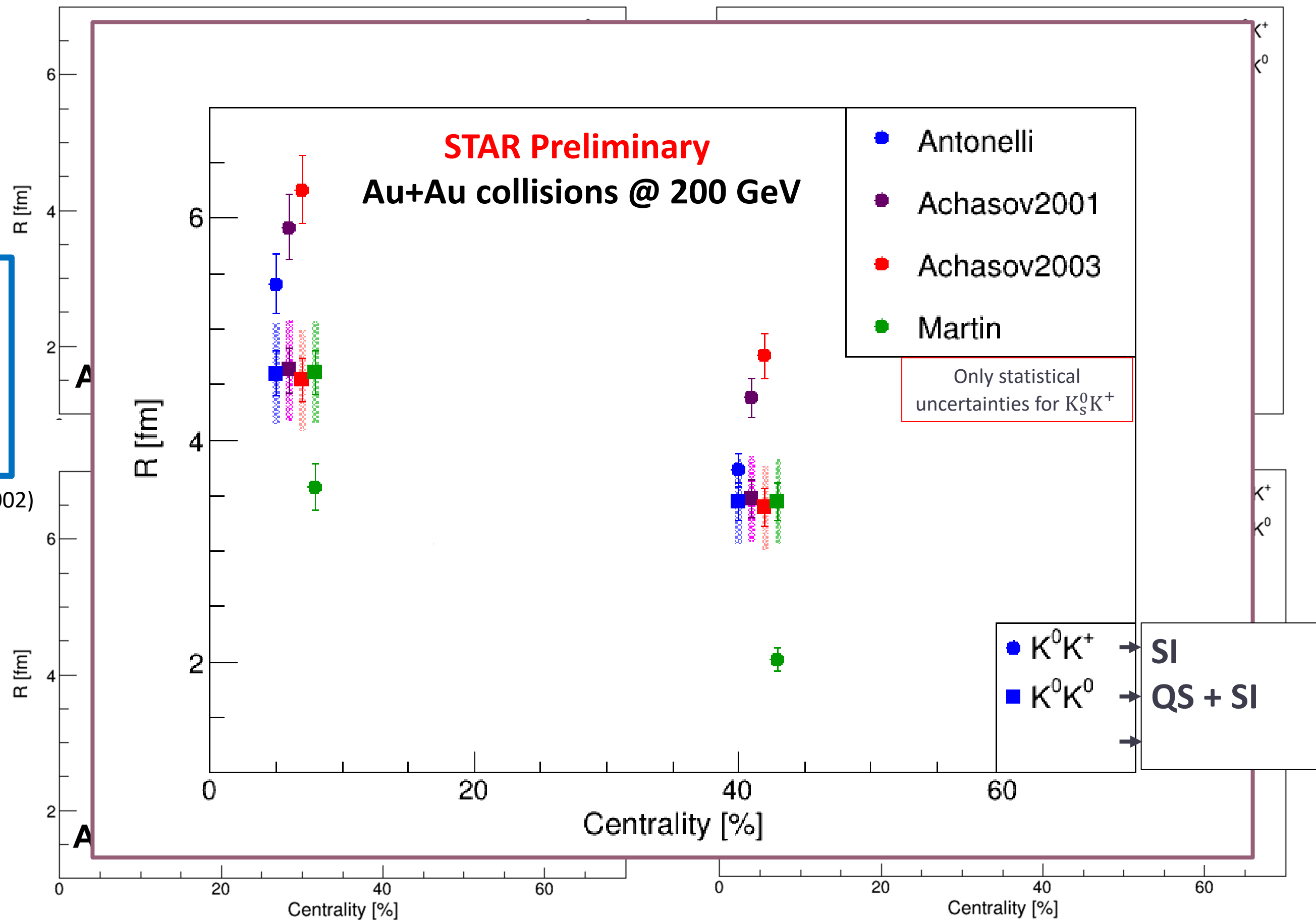


Antonelli
favors a_0
resonance as
a tetraquark

eConf C020620, THAT06 (2002)



Comparison - $K_S^0 K_S^0$ and $K_S^0 K^+$ - 200 GeV



Antonelli
favors a_0
resonance as
a tetraquark

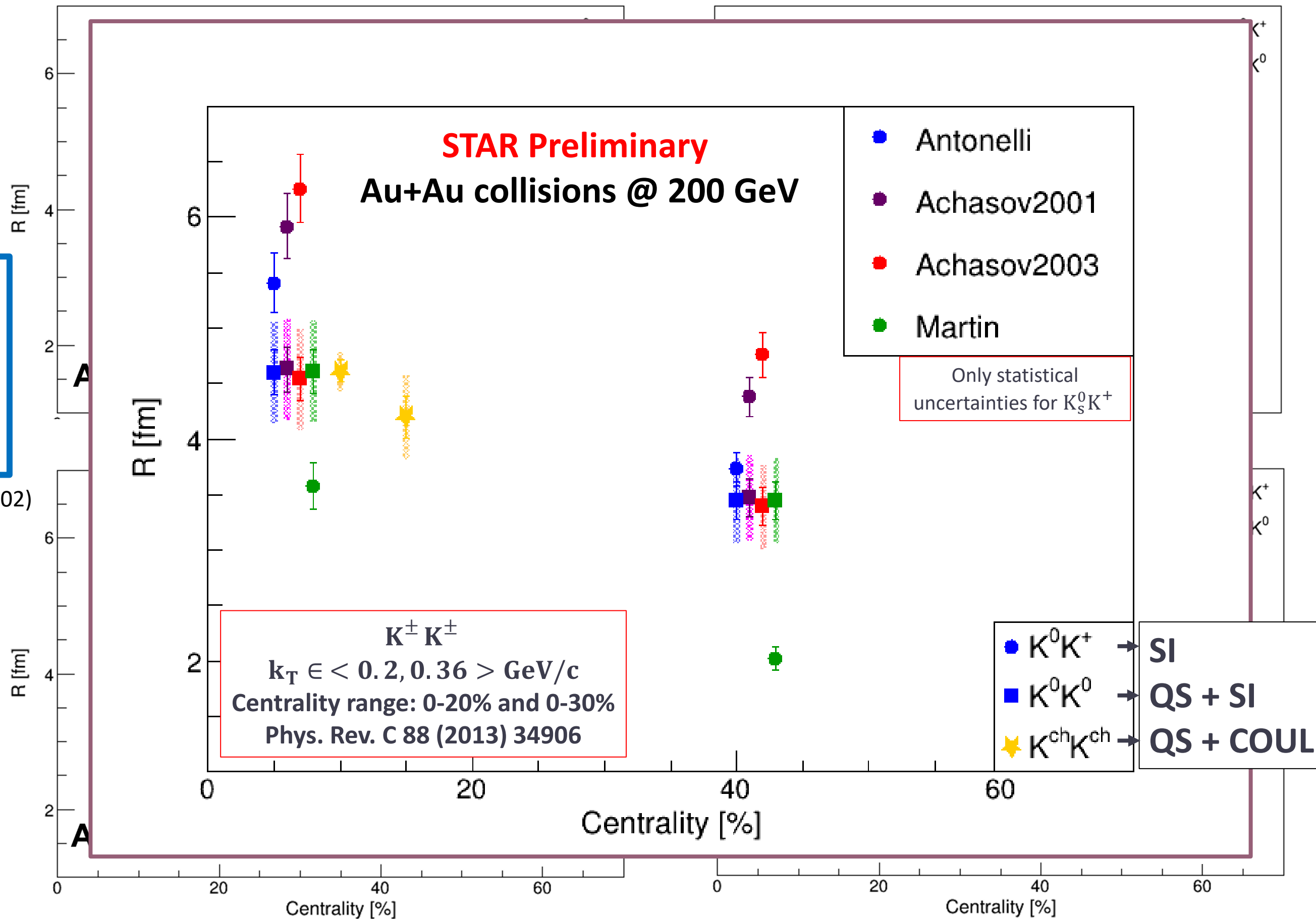
eConf C020620, THAT06 (2002)



Comparison - $K_S^0 K_S^0$ and $K_S^0 K^+$ - 200 GeV

Antonelli
favors a_0
resonance as
a tetraquark

eConf C020620, THAT06 (2002)



$$R_{K^\pm K^\pm} = \sqrt{\frac{R_{out}^2 + R_{side}^2 + R_{long}^2}{3}}$$



Summary

$K_S^0 K_S^0$ femtoscopy

- The strong final-state interaction has a significant effect on the $K_S^0 K_S^0$ correlation due to the near-threshold $f_0(980)$ and $a_0(980)$ resonances
- The radii of the source depend on centrality and increase with increasing collision energy
- Extracted source radii are comparable to these from models

$K_S^0 K^+$ femtoscopy

- The $a_0(980)$ FSI parametrization gives very good representation of the shape of the signal region in CF
- The parametrization with the larger $a_0(980)$ mass and decay coupling gives larger size of the source
- Comparison with $K_S^0 K_S^0$
 - Antonelli parametrization favors $a_0(980)$ resonance as a tetraquark



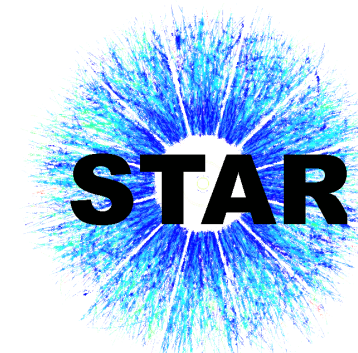
Summary

$K_S^0 K_S^0$ femtoscopy

- The strong final-state interaction has a significant effect on the $K_S^0 K_S^0$ correlation due to the near-threshold $f_0(980)$ and $a_0(980)$ resonances
- The radii of the source depend on centrality and increase with increasing collision energy
- Extracted source radii are comparable to these from models

$K_S^0 K^+$ femtoscopy

- The $a_0(980)$ FSI parametrization gives very good representation of the shape of the signal region in CF
- The parametrization with the larger $a_0(980)$ mass and decay coupling gives larger size of the source
- Comparison with $K_S^0 K_S^0$
 - Antonelli parametrization favors $a_0(980)$ resonance as a tetraquark



Summary

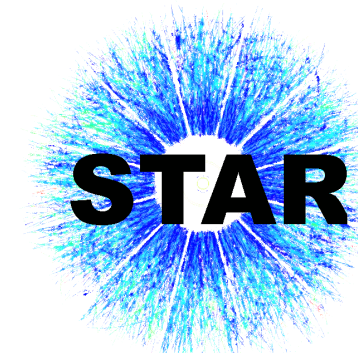
$K_S^0 K_S^0$ femtoscopy

- The strong final-state interaction has a significant effect on the $K_S^0 K_S^0$ correlation due to the near-threshold $f_0(980)$ and $a_0(980)$ resonances
- The radii of the source depend on centrality and increase with increasing collision energy
- Extracted source radii are comparable to these from models

$K_S^0 K^+$ femtoscopy

- The $a_0(980)$ FSI parametrization gives very good representation of the shape of the signal region in CF
- The parametrization with the larger $a_0(980)$ mass and decay coupling gives larger size of the source
- Comparison with $K_S^0 K_S^0$
 - Antonelli parametrization favors $a_0(980)$ resonance as a tetraquark

Compatibility of source sizes for $K_S^0 K_S^0$, $K_S^0 K^+$ and $K^\pm K^\pm$ pairs in the case of Antonelli



Summary

$K_S^0 K_S^0$ femtoscopy

- The strong final-state interaction has a significant effect on the $K_S^0 K_S^0$ correlation due to the near-threshold $f_0(980)$ and $a_0(980)$ resonances
- The ratio of the correlation function to the uncorrelated case with increasing $\sqrt{s_{NN}}$ increases
- Extracted source sizes are smaller than for $K_S^0 K_S^0$ femtoscopy
- The $a_0(980)$ resonance is the dominant contribution to the shape of the correlation function
- The parameter α is smaller than for $K_S^0 K_S^0$ femtoscopy, which gives larger size of the source
- Comparison with $K_S^0 K_S^0$
 - Antonelli parametrization favors $a_0(980)$ resonance as a tetraquark

Outlook

High statistic BES-II data give the ability to analyze neutral kaon femtoscopy for energies $\sqrt{s_{NN}} < 20$ GeV

Compatibility of source sizes for $K_S^0 K_S^0$, $K_S^0 K^+$ and $K^\pm K^\pm$ pairs in the case of Antonelli



Thank you for your attention!!

